Characterization of DNA Duplex Structure, Stability and Formation Kinetics in a Eutectic Solvent and Its Aqueous Mixtures

A Thesis
Presented to
The Academic Faculty

By

Brandon P. Laughlin

In Partial Fulfillment
of the Requirements for the Degree
Master of Science in the
School of Chemistry and Biochemistry

Georgia Institute of Technology
December 2014

Characterization of DNA Duplex Structure, Stability and Formation Kinetics in a Eutectic Solvent and Its Aqueous Mixtures

Approved by:

Dr. Nicholas V. Hud, Advisor
School of Chemistry and Biochemistry
Georgia Institute of Technology

Dr. Loren D. Williams
School of Chemistry and Biochemistry
Georgia Institute of Technology

Dr. Roger Wartell
School of Biology
Georgia Institute of Technology

Date Approved: November 14, 2014

ACKNOWLEDGMENTS

I would first like to thank Dr. Nicholas Hud for supporting me throughout my time at Georgia Tech, through good and bad, even as I made my switch from the PhD track to a Master's degree. You've been infinitely patient with me and I thank you for it.

Dr. Isaac Gallego, Christine He, and Dr. Martha Grover are all deserving of my thanks as well for their contributions to this work, and for helping me whenever I needed it, even when I wasn't aware I did!

Brian Cafferty, David Fialho, Ford Lannan, Timothy Lenz, Irena Mamajanov, Caterina Musetti, Denise Okafor, and Chelsea Walker, thank you for making the day to day life in lab as enjoyable is it was.

I would also like to thank the NSF for providing the funding for the CCE, and therefore this project and myself, and the laboratory of Dr. Victor Breedveldt for allowing the use of their viscometer and the assistance to go with it.

And to Po-Yi, your tolerance of me is superhuman, and I can't express enough my feelings of gratitude for you stickin' around. 我愛你!

TABLE OF CONTENTS

LIST OF TABLES

LIST OF FIGURES

SUMMARY

In this work, properties and behavior of DNA oligonucleotides in a non-aqueous eutectic comprised of glycerol and choline chloride mixed at varying ratios, as well as aqueous mixtures of the eutectic are explored. Physical parameters of buffer-containing eutectics such as density and viscosity at 293 K are determined. The effects the eutectic have upon the stability of the duplex formation of an oligonucleotide through melting and reannealing relative to that in a buffer are determined, and thermodynamic parameters also derived. It is found that the oligonucleotides explored form stable duplex structures in all investigated conditions. Structural studies by circular dichroism spectroscopy of the oligonucleotides have also been done, and show the subtle effects on DNA secondary structure alterations of the eutectic composition can have, with all conditions maintaining a B-form structure. Finally, the rate constants of the annealing reaction of the two complementary strands are determined through monitoring recovery of duplex structure after heating and rapid cooling.

1 INTRODUCTION

Water is often seen as a necessary solvent component for structural integrity of oligonucleotide secondary structure.[1] A non-aqueous solvent could provide potential for completely different chemistry, however, the hydrophilic nature of nucleotides renders them insoluble in organic solvents without additional modification.[2] This organic insolubility is in fact commonly used in laboratories as a means of precipitating DNA for purification via the addition of alcohols. Potentially hydrophilic anhydrous solvents, in the form of eutectics, exist that could avoid precipitation. Eutectics are typically comprised of a hydrogen bond donor and acceptor, such as two organics or salts, that when combined result in a drastically lower melting temperature relative to the individual components. This can create a liquid at room temperature from what was originally two solids.[12] These eutectics can offer unique environments for study due to their potential as solvents with properties distinct from most other organic or aqueous solvents.

Our laboratory has previously demonstrated the viability of stable nucleic acid secondary structures in deep eutectic solvents[6]. In this earlier work, a urea and choline chloride eutectic was the solvent of choice. While in this solvent, most DNA duplexes adopted an A-form structure, unlike the B-form typically found in the conditions of living cells and buffered solutions.[3] Urea can also pose issues with stability of other folded biopolymers such as proteins. As eutectics have been shown to provide an environment

that permits enzymatic reactions, finding conditions that are anhydrous but support biopolymer structures as similar to water as possible is of interest.[45] In order to determine if there are anhydrous conditions under which DNA is capable of maintaining a B-form structure despite the lack of water, other eutectics were explored.

A eutectic comprised of glycerol and choline chloride was first investigated by the Abbott laboratory[7], where it was made with a wide range of glycerol : choline chloride molar ratios. Prasad et al. also demonstrated that salmon testes DNA will dissolve directly into a glycerol : choline chloride mixture and retain a stable B-form structure over long time periods after recovery into buffer, suggesting that eutectics could be utilized for storage and chemical derivatization[8]. We therefore explored the structural behavior of DNA oligonucleotides in the eutectic to determine if the B-form is present while in the solvent, as well as the thermal stability of the double stranded structure, and how they change as water is added or removed from the environment. Choline chloride in particular is an interesting molecule in this context, as the quaternary amine can potentially provide groove-binding behavior similar to that of polyamines, such as spermine.[43]

A feature of eutectics that often differs from water is the high viscosity of the anhydrous solution. Given Kramer's Theory, as seen below, any diffusion limited process, including the annealing of separated strands of oligonucleotides, could exhibit differing behavior in these viscous solvents when compared to water. In the 1970s, Wetmur et al concluded[26] that the viscosity dependent rate-limiting step of annealing

was that of the formation of the second base pair after nucleation and not a diffusion dependent characteristic. Schmitz and Schurr[27] then challenged their conclusion and asserted that thermal DNA renaturation was indeed diffusion controlled. Thrower and Peacocke claimed that the rate controlling step of the reannealing of large strands of E. coli DNA is the diffusion of the strands and the nucleation of the duplex region.[37] To this day, the exact workings of the mechanism remain unsolved[9].

$$k_{nu} = \frac{BN^{-\nu\theta 2}}{\eta}$$

Our laboratory has demonstrated in the past the effects viscosity can have upon the rearrangement of a G-quadruplex[10]. In that work, it was found that viscosity enabled the molecule to enter a kinetically trapped state it could not access in low viscosity conditions. In this work small oligonucleotide annealing after thermal denaturation is further explored.

Subriana and Doty noted[28] that macromolecular cosolutes had little effect on the reannealing rates of T4 DNA, while sucrose did, indicating that macro-scale viscosity does note affect the reannealing process, while smaller solvent components may increase viscosity on the nanometer scale. Weider and Wetmur found that macromolecular cosolutes actually increased the reannealing rate of DNA, likely through volume exclusion effects that increase the effective concentration of the DNA.[40] These volume exclusion effects are not likely to be active in small-molecule based solvents.

Oligonucleotide behavior in eutectics is also of interest in the search for

potential alternative solvents that could answer questions about the chemistry of the origins of life[4]. The problem of a water based environment in synthesizing stable nucleotides and forming bonds between them has motivated this hypothesis. Mixtures of eutectic solvents in water have been proposed as a possible environment for the early development of life, as water drying off from evaporation will concentrate the eutectics and minimize water activity, while still providing a liquid medium within which chemistry could occur.[5]

A better understanding of anhydrous solvents for nucleotides is also of interest for DNA nanotechnology. The complex origami structures created by engineering specific folding of DNA are dependent upon buffered conditions and rely on B-form architecture. DNA origami under non-aqueous conditions has only been achieved through use of surfactant complexes after prior folding in hydrated conditions.[44] An anhydrous system that can support the B-form structure open the door to new chemistries with DNA nanotechnology.

Encouraged by our past work with eutectics and the information in the literature, we have set out to better characterize the behavior and properties of oligonucleotides in the glycerol : choline chloride eutectic solvent.

2 EUTECTIC CHARACTERIZATION

2.1 Introduction

The initial experimental work to be done was characterization of the glycerol : choline chloride eutectic. The work by Abbott et al[7] has demonstrated numerous properties of the eutectic ranging up to a glycerol : choline molar ratio of up to 1 ; 0.33, but for our purposes more characterization was necessary, as their study explored a smaller range of glycerol : choline chloride ratios than was determined to be available. We were also interested in investigation of the aqueous mixtures of the eutectic, while Abbott only discussed water-free eutectics. In addition, their work was done at 298.15 K, while ours was to be done at 293.15 K. Our goal is to establish that a wide range of conditions are available, allowing tunability to specific viscosities or desired properties of nucleic acids given different ratios of the eutectic components and their dilution with water at various ratios.

An important feature for the hypothesis of utilizing heating/cooling cycles for separating and annealing complementary strands is the assumption that the eutectic components in aqueous solution will remain in liquid form while water evaporates, allowing cycling between an aqueous solution and a water-free eutectic. Testing for the volatility of the eutectic to ensure that any mass loss under conditions allowing for loss of water are either not present or minimal was therefore a necessary early step in exploring the use of this eutectic.

It should also be noted that the glycerol : choline chloride eutectic explored

here is not proposed to be the only anhydrous solvent capable of supporting the B-form structure. There are many eutectics, and while not all support stable DNA secondary structures, it is known that some do, and there are many more that can be explored.

2.2 Materials and Methods

2.2.1 Eutectic Preparation

Glycerol (Alfa Aesar, ACS, 99.5%) was dried under vacuum at 140 mTorr. Choline chloride (Alfa Aesar, ≥98%) was recrystallized in ethanol, filtered, and dried under vacuum. To prepare the eutectics, an analytical balance was used to measure amounts of glycerol and the required mols of choline chloride for each desired solvent ratio, followed by vortexing and placing the mixtures in an oven at 75 °C until a clear liquid was formed. Eutectics with higher concentrations of choline chloride required vortexing every few hours during heating to ensure no precipitate would form after returning them to room temperature. The eutectics were then placed under vacuum of 140 mTorr overnight and stored in a desiccator.

2.2.2 Sample Preparation

Eutectics were transferred into microcentrifuge tubes and weighed on an analytical balance. The volume of buffer and water needed for each sample were calculated from this measurement. Sodium phosphate buffer, pH 7, was added to the volume required for a final concentrations of 20 mM. The samples were then placed in a Centrivap vacuum concentrator for twelve hours. Next, nanopure water was added to the appropriate samples and briefly vortexed at ten minute intervals while

sitting at 37 °C until the samples were homogenous.

2.2.3 Density Measurements

Samples were pipetted at 100 µL volumes on an analytical balance using a calibrated Gilson Microman viscous pipette at 20 °C.

2.2.4 Determination of Rate of Mass Loss Under Vacuum

50 mg of water was added to 250 mg of each eutectic ratio and placed in a Centrivap vacuum concentrator. Freshly prepared eutectic was used as a control. The mass of each sample was monitored over a twelve-hour period using an analytical balance.

2.2.5 Viscosity Measurements

A MCR300 rheometer was used for the viscosity measurements. 125 µL of eutectic was used for each reading, with measurements taken at 20 °C. An average of five readings per sample was used to determine the viscosity.

2.3 Results and Discussion

2.3.1 Determination of Eutectic Composition

The initial work to be done was to determine the range of glycerol : choline chloride ratios available. Abbott's work had previously demonstrated up to 1 mol glycerol : 0.33 mol choline chloride, but no indication was given of that being an upper limit. In our preparations, we found that choline chloride is soluble in the glycerol up to a ratio of 1 mol glycerol : 0.80 mol choline chloride. This ratio is the observed upper limit of possible molar ratios, as it requires extremely thorough

mixing and heating to ensure that the components not only dissolve together, but the choline chloride does not precipitate out of solution while at room temperature. Solutions of this particular glycerol : choline chloride ratio were found to be stable for at least three months if no solid precipitate is present and the solvent is heated and mixed thoroughly, and will typically form precipitate overnight if not. Higher ratios were found to have insoluble choline chloride precipitate present regardless of how much heating or vortexing was done. Sonication did not expand the range of molar ratios possible for the eutectic solvent. Given this maximum, we focused on solvents with glycerol : choline chloride molar ratios of 1:0.05, 1:0.20, 1:0.35, 1:0.50, 1:0.65, and 1:80. For the addition of water, 0%, 3%, 7%, 10%, 20%, 35%, 50%, 80%, and 95% mol percentage water was settled on for the dilutions of each of the six eutectic ratios. For the purpose of calculating the various molar ratios, moles of eutectic are determined by adding together the total moles of glycerol and choline chloride. This allows for a range of measurements from nearly water like solution to a water free eutectic, with a focus on the higher eutectic concentrations that may have more of an effect on the behavior of the DNA.

2.3.2 Density Measurements of Eutectic and Aqueous Eutectic Mixtures

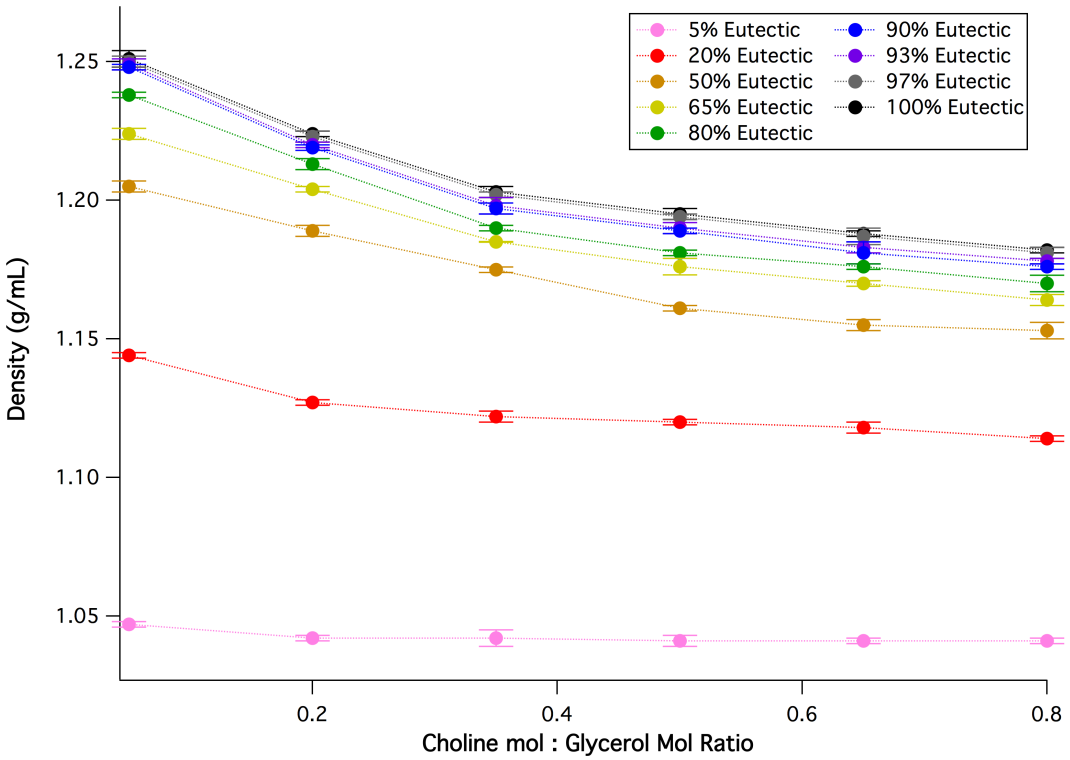

Figure 2.1 Density of glycerol:choline chloride eutectics at 20 °C. All percentages are molar and diluted with water

Table 2.1 Density of glycerol : choline chloride eutectic at 20 °C. All percentages are molar and diluted with water.

Glycerol : Choline Mol Ratio

Density (g/mL)	1 : 0.80 G:C	1 : 0.65 G:C	1 : 0.50 G:C
5% Eutectic	1.041	1.041	1.041
20% Eutectic	1.114	1.118	1.121
50% Eutectic	1.153	1.155	1.161
65% Eutectic	1.164	1.170	1.176
80% Eutectic	1.170	1.176	1.181
90% Eutectic	1.176	1.181	1.189
93% Eutectic	1.178	1.183	1.190
97% Eutectic	1.180	1.187	1.194
100% Eutectic	1.181	1.187	1.194

Density (g/mL)	1 : 0.35 G:C	1 : 0.20 G:C	1 : 0.05 G:C
5% Eutectic	1.042	1.042	1.047
20% Eutectic	1.122	1.127	1.144
50% Eutectic	1.175	1.189	1.205
65% Eutectic	1.185	1.204	1.224
80% Eutectic	1.190	1.213	1.238
90% Eutectic	1.197	1.219	1.248
93% Eutectic	1.198	1.220	1.249
97% Eutectic	1.202	1.223	1.250
100% Eutectic	1.203	1.224	1.251

In order to be able to prepare the range of samples to the correct concentrations and ratios, the varying eutectic mixtures first needed to have their densities determined. Although pipettes designed for work with viscous liquids are

available, it can still be difficult to accurately reproduce volumes, and so weighing the mass of samples after pipetting is the ideal method for calculating volume present from the densities of the eutectics. The results are displayed in Figure 2.1 and Table 2.1. The range of eutectic density is between that of water (1 g/mL) and pure glycerol (1.26 g/mL), increasing in density as glycerol content increases and reducing in density as choline chloride and water content increases. The values reached are in good agreement with recently published values[11].

2.3.3 Volatility of Eutectics and Aqueous Eutectic Mixtures Under Vacuum

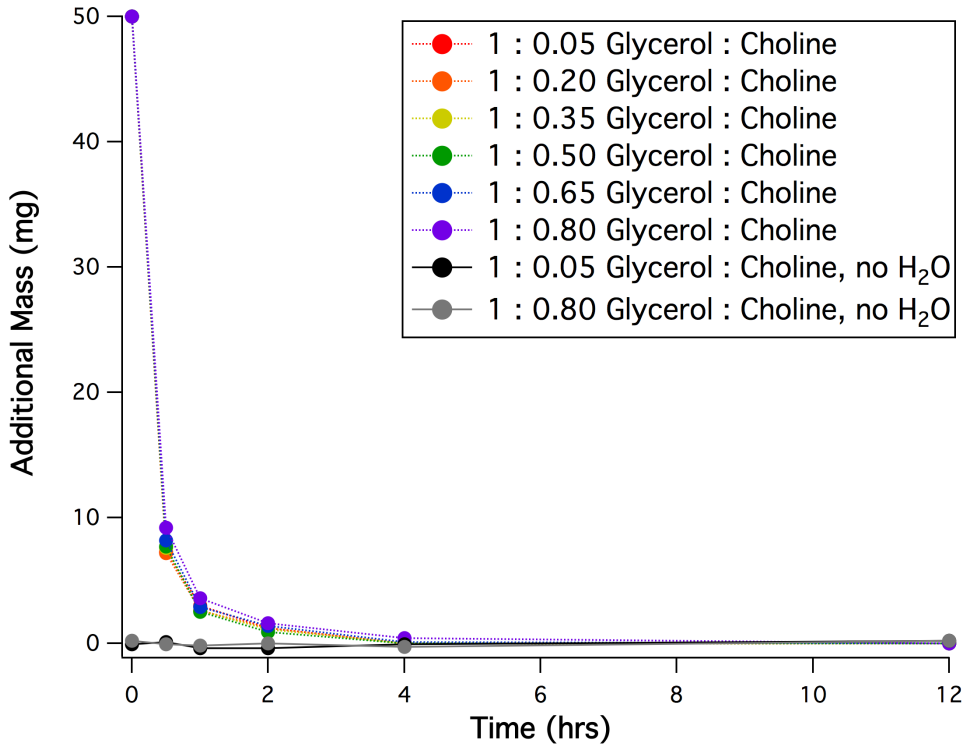

Figure 2.2 Loss of additional mass added to glycerol : choline chloride eutectics as water. Samples were placed in a vacuum concentrator at 130 mTorr and monitored through weighing on an analytical scale to track volatility of eutectic and water dissolved in eutectic.

The volatility of the solvents was then investigated to ensure that sample

preparation had been and would be accurate and reproducible, because a necessary step of the process of preparing the samples is to dry off any water that was either initially present in the eutectic or had been added along with the phosphate buffer or DNA. 250 mg of each of the different eutectic ratios was prepared and 50 mg of H_2O then added to the samples and left to dissolve together for one hour with vortexing at the half hour mark. The samples were then subjected to a vacuum of 140 mtorr. The samples showed >99% loss of 50 mg of mass after two hours, and complete loss of 50 mg by 12 hours, Figure 2.2. Control samples of eutectics showed no similar loss of mass over the twelve-hour period, displaying their lack of volatility relative to that of water.

Karl-Fisher analysis confirms the loss of water after the vacuum drying process, with results showing less than 0.1% of water remaining.

2.3.4 Viscosity Measurements of Eutectics and Aqueous Eutectic Mixtures

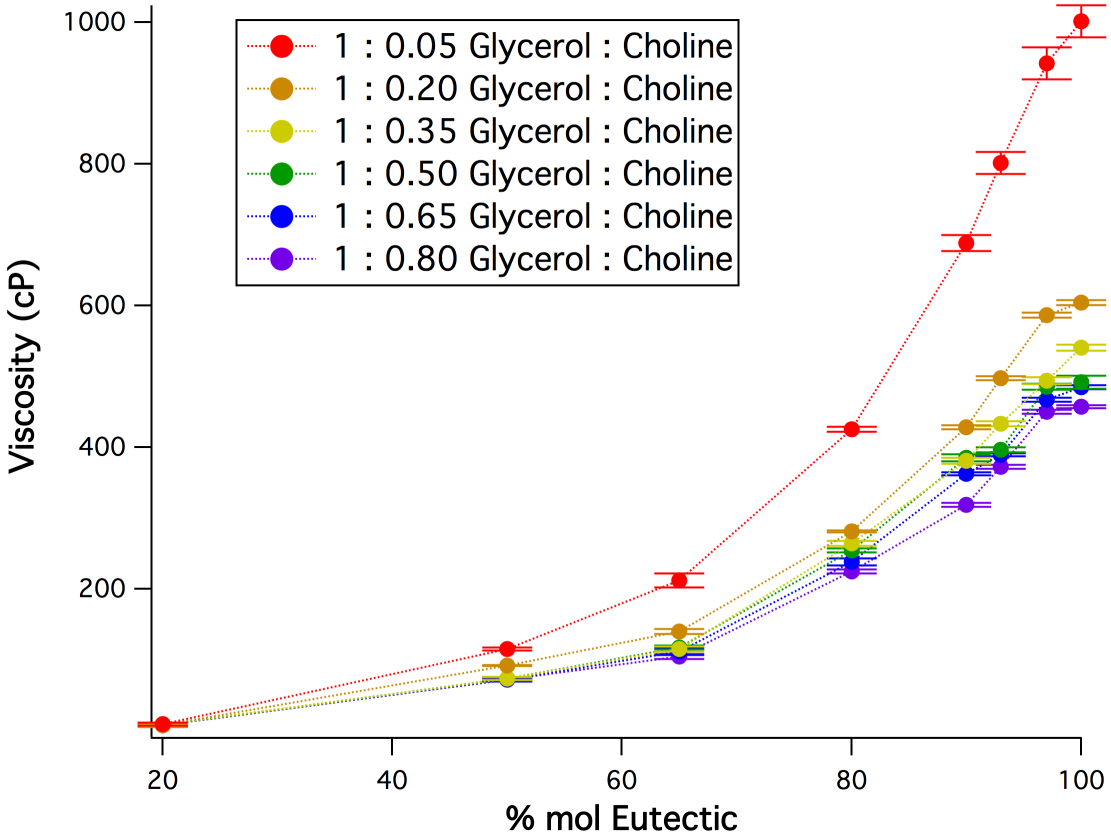

Figure 2.3 Viscosity of glycerol:choline chloride eutectics at 20 °C as a function of mol % eutectic, diluted with H_2O

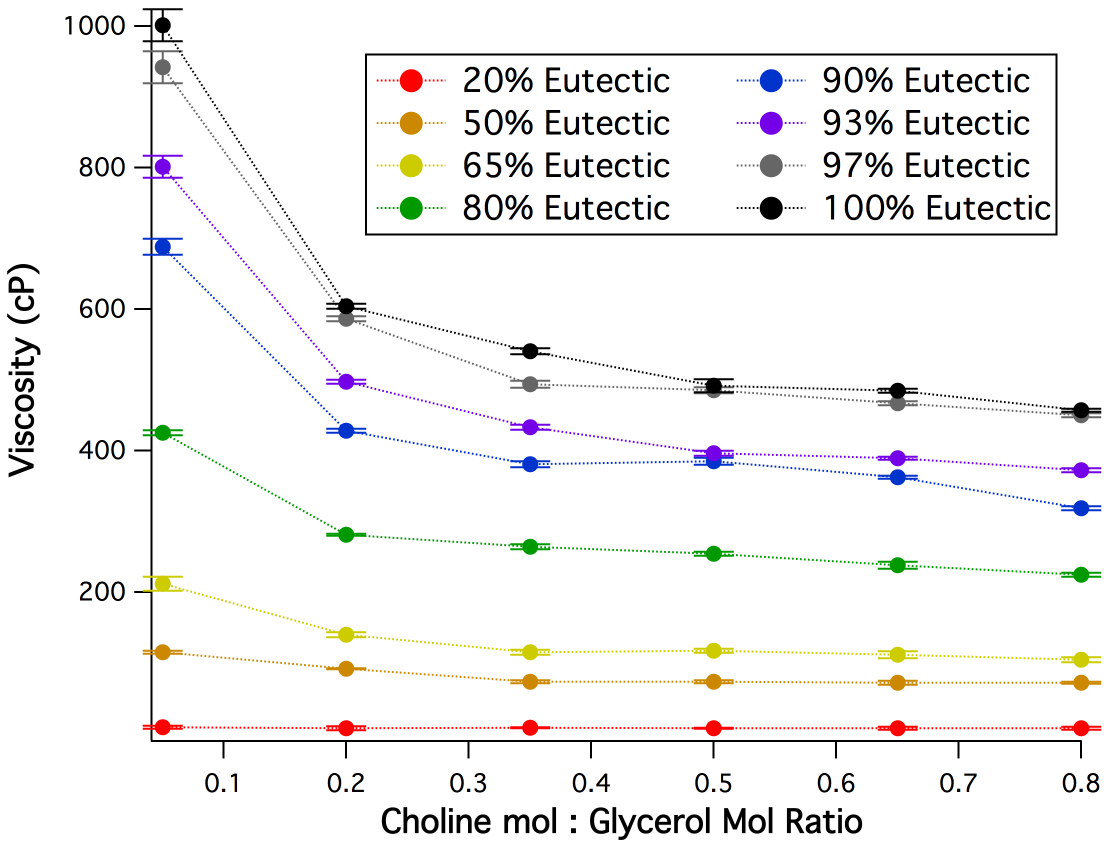

Figure 2.4 Viscosity of glycerol : choline chloride eutectics at 20 °C as a function of the glycerol : choline chloride molar ratio

Table 2.2 Viscosities of glycerol:choline chloride eutectics at 20 °C. All percentages are molar and diluted with water.

Glycerol : Choline Mol Ratio

Viscosity (cP)	1 : 0.80	1 : 0.65	1 : 0.50
20% Eutectic	7.6±1.9	7.2±2.0	7.4±0.9
50% Eutectic	71.6±1.5	71.6±2.7	73.3±2.0
65% Eutectic	103.9±3.3	111.1±4.7	116.8±2.9
80% Eutectic	224.4±3.1	237.8±4.9	253.8±2.6
90% Eutectic	318.4±2.6	362.2±1.9	384.8±4.9
93% Eutectic	372±2.8	389.2±1.8	396±3.5
97% Eutectic	450±2.6	467±2.7	485±4.5
100% Eutectic	456.8±1.9	484.6±2.8	491.4±9.1

Viscosity (cP)	1 : 0.35	1: 0.20	1 : 0.05
20% Eutectic	7.9±0.6	7.2±2.7	8.8±1.9
50% Eutectic	72.9±2.4	91.2±0.6	115±2.4
65% Eutectic	114.7±3.9	139.6±3.8	212±10.2
80% Eutectic	264±3.8	281±1.6	425±3.8
90% Eutectic	380.8±4.3	428.2±2.6	688±11.3
93% Eutectic	433.2±3.8	497.4±3.0	801.2±15.4
97% Eutectic	493.8±5.3	586.4±4.0	942±22.8
100% Eutectic	540.2±4.0	604±3.4	1001.4±22.6

The high viscosity of this eutectic solvent is of particular interest for using solvent properties as a means to alter nucleic acid folding/assembly Measured viscosity values are shown in Figures 2.3 and 2.4, and Table 2.2. The 5% eutectic dilution proved too low in viscosity to be accurately measured, probably having a

viscosity between the 1 cP of water at 20 °C and the roughly 7.5 cP displayed among the 20% eutectic mixtures, which were capable of measurement. The results demonstrate how alteration of the glycerol : choline chloride ratio and the addition of water makes a large range of viscosities available for use, from the nearly water like values of the 20% eutectic to a peak value of two orders of magnitude greater in the 100% 1:0.05 eutectic. The observed drop in viscosity in the eutectics seen from the addition of greater amounts of choline chloride is likely due to disruption of the intermolecular glycerol interactions that lead to the high viscosity seen in pure glycerol[12]. The largest change seen in Figure 2.3, between that of 1 : 0.05 and 1 : 0.20 glycerol choline chloride is not surprising, as this change ratios correlates with the greatest change in choline chloride molarity, with a 105.5% increase in molarity in the 100% eutectic from 1 : 0.05 to 1:0.20, to a 37.9% increase in the jump from 1 : 0.20 to 1 : 0.35. Figure 2.4 clearly shows this behavior, as a large drop can be seen after the first set of eutectics, to a more gradual decrease between ratios after that as choline chloride content increases.

3 THERMAL MELTING OF OLIGONUCLEOTIDES IN EUTECTIC SOLVENTS

3.1 Introduction

DNA is known to form stable secondary structure in certain eutectic solvents[6][10], and an increasing number of publications are exploring other DNA structures in eutectic solvents, such as G-quadruplexes[13]. We wished to determine how the changing glycerol : choline chloride ratios and eutectic concentrations would alter the stability of the DNA duplex.

A comparison of DNA duplex stability in standard of aqueous buffers to non-aqueous conditions, such as glycerol, typically reveals a significant reduction in stability,[14] as measured by thermal denaturation studies.

Oligonucleotides in glycerol solvents and their dilutions were also explored, to investigate how the presence of the choline component of the solutions altered the properties of the oligonucleotides relative to pure glycerol.

The hyperchromic effect was utilized to monitor the stability of a DNA duplex. This phenomenon is the increase in absorbance observed at 260 nm as oligonucleotides bases are freed from stacking interactions, shifting from a double stranded form to unassociated single stranded forms. Changes in absorbance such as this are the simplest means of monitoring the hybridization state of complementary DNA strands.[15]

In this and the following studies, the DNA strands were designed specifically to minimize self-complementarity and eliminate multiple repeats of the same base. Tracts of a single base are known to change both stability and structural behavior of an oligonucleotide, and so a mixed sequence was chosen to best model what a random sequence would behave like.[42]

3.2 Materials and Methods

3.2.1 DNA Preparation

Oligonucleotides were purchased from Integrated DNA Technologies and used as delivered after resuspension in nanopure H_2O and quantification.

32-mer A	d(GGT GTC AGT AAG CCA TTC GAG ATC CTC ATA GT)
32-mer B	d(ACT ATG AGG ATC TCG AAT GGC TTA CTG ACA CC)
Hairpin (HP18)	d(GCA AAA CGA AGT TTT GC)

3.2.2 Sample Preparation

Samples were prepared similar to the eutectic preparation described in Section 2.2.2, but with the addition of oligonucleotides as well. DNA was added at the same time as the phosphate buffer to a volume required for a final concentration of 250 μg/mL by base DNA (12.36 μM by strand for dsDNA, 46.53 μM for HP18). Each solution was transferred into a 1 mm strain-free quartz cuvette via centrifugation and heat cycled from room temperature to 90 °C and back to ensure homogeneity.

3.2.3 Oligonucleotide Melting Points

The samples were taken to a Cary 50 UV-Vis spectrophotometer and scanned

from 20 °C to 90 °C for the eutectic samples, and 10 °C to 90 °C for the glycerol samples. The peak at 260 nm was tracked, and baseline corrections were applied to the upper and lower regions of the melt, corresponding with melted and annealed DNA respectively. The median was taken between the baselines and used to determine the melting temperature.

3.2.4 Oligonucleotide Thermodynamic Values

The melting data was converted to association constants and fit with the Van't Hoff equation. The slope was used to calculate the $\Delta H°$, the intercept to determine $\Delta S°$, and the relationship of $\Delta G° = \Delta H° - T\Delta S°$ to determine the Gibbs free energy at 37 °C.

3.3 Results and Discussion

3.3.1 Oligonucleotide Stability in the Eutectic and Aqueous Eutectic Mixtures

Figures 3.1 through 3.9 show the melting curves for the oligonucleotide in the range of eutectics explored. The solid line represent the average of the three curves shown, while the dotted lines are the three individual melts. The resulting melting temperatures are summarized in Table 3.1.

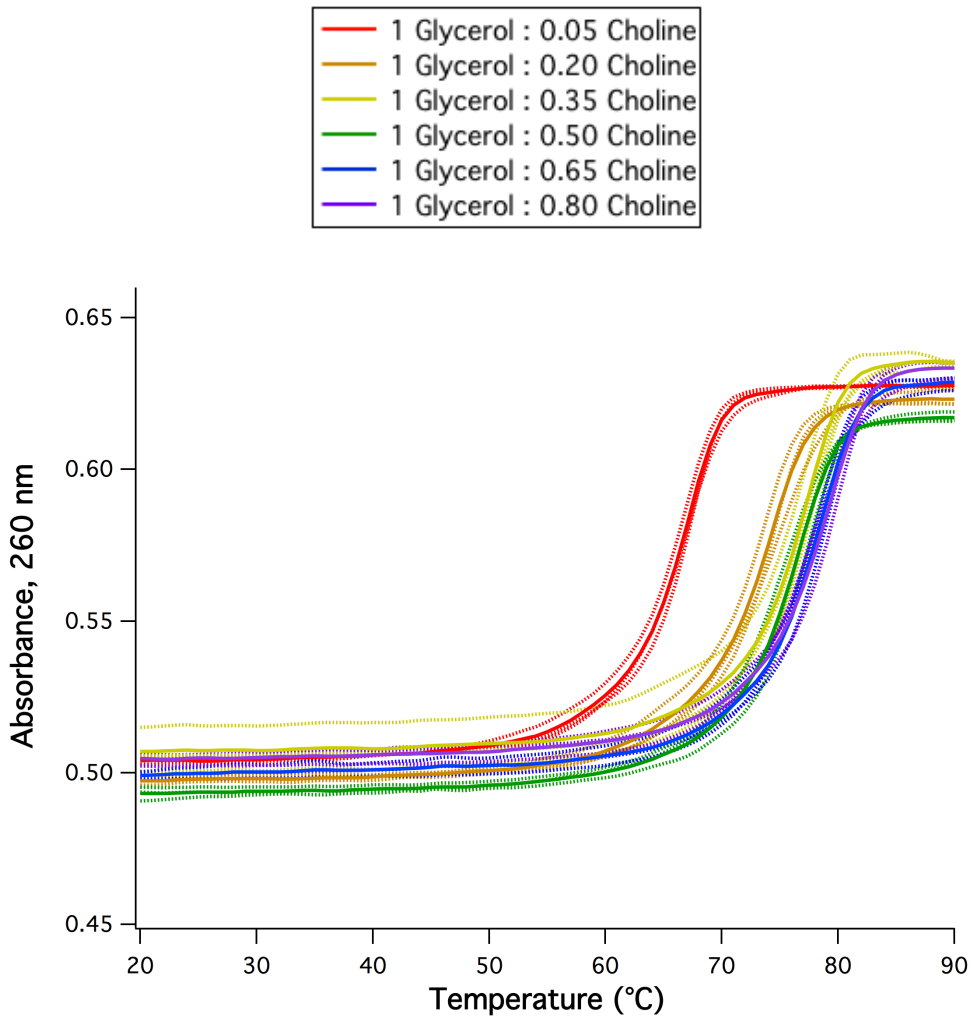

Figure 3.1 Melting traces of 32-mer DNA duplex (250 µg/mL) in 5% mol eutectic

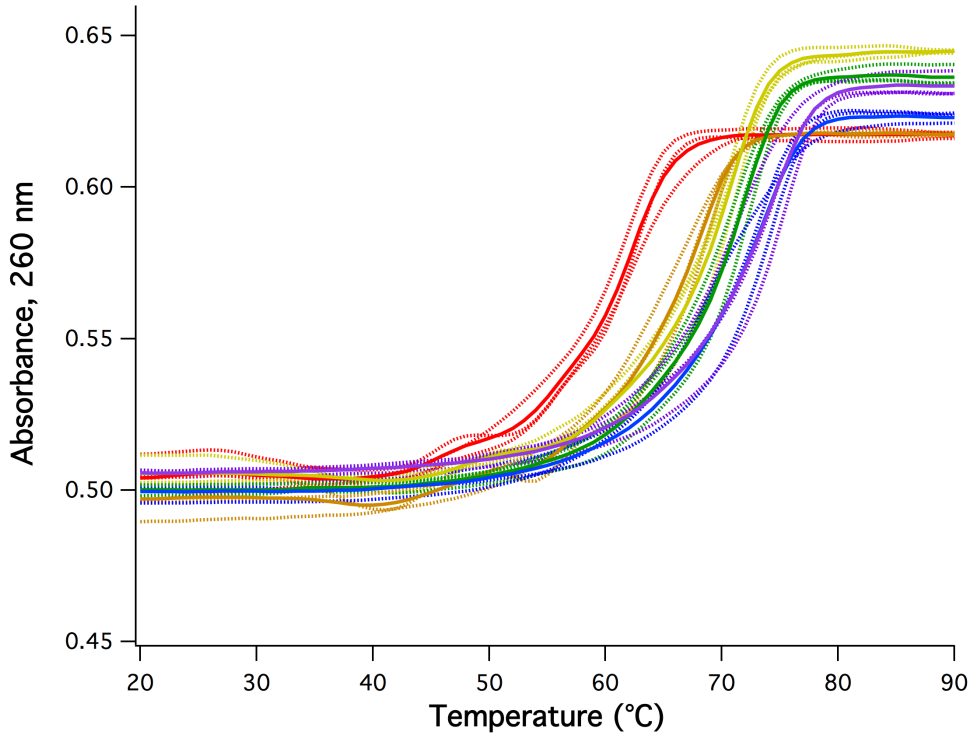

Figure 3.2 Melting traces of 32-mer DNA duplex (250 μg/mL) in 20% mol eutectic

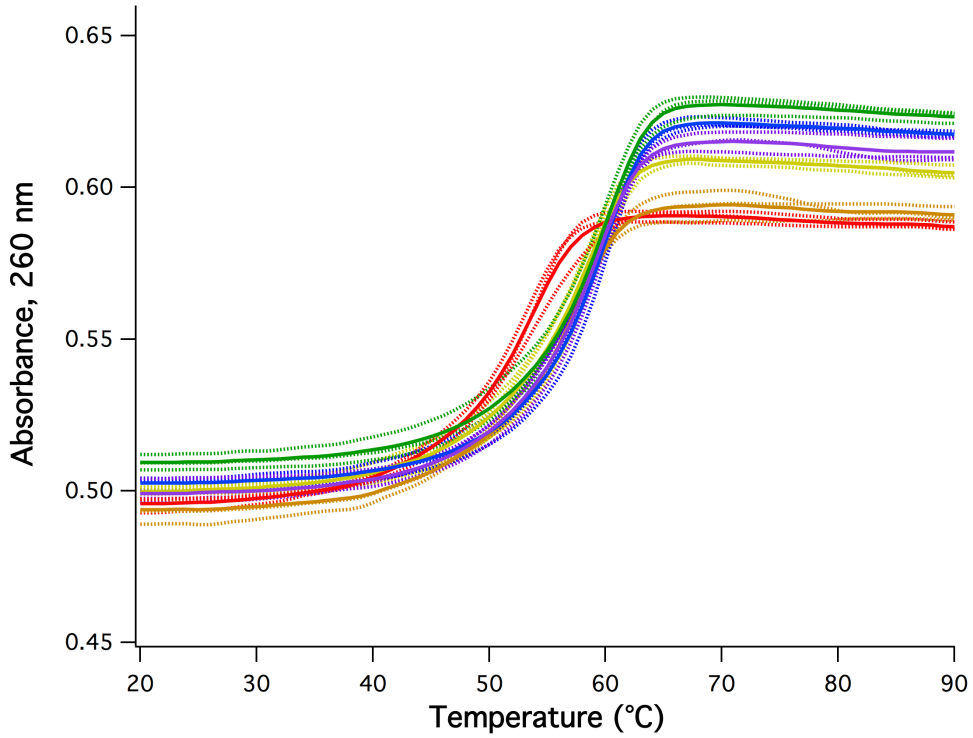

Figure 3.3 Melting traces of 32-mer DNA duplex (250 μg/mL) in 50% mol eutectic

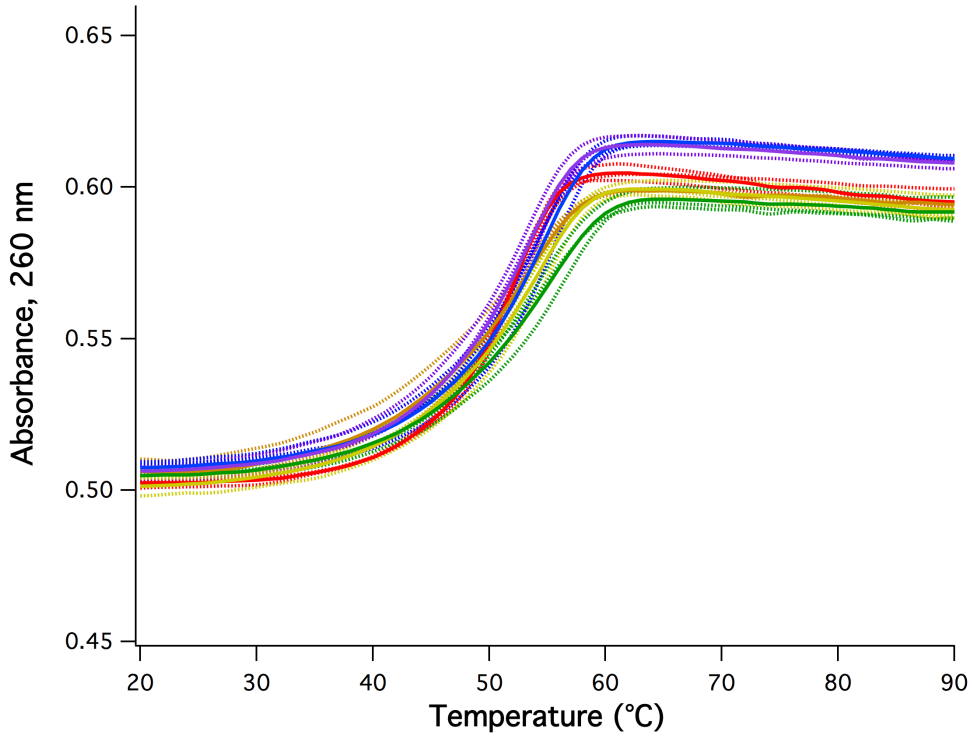

Figure 3.4 Melting traces of 32-mer DNA duplex (250 μg/mL) in 65% mol eutectic

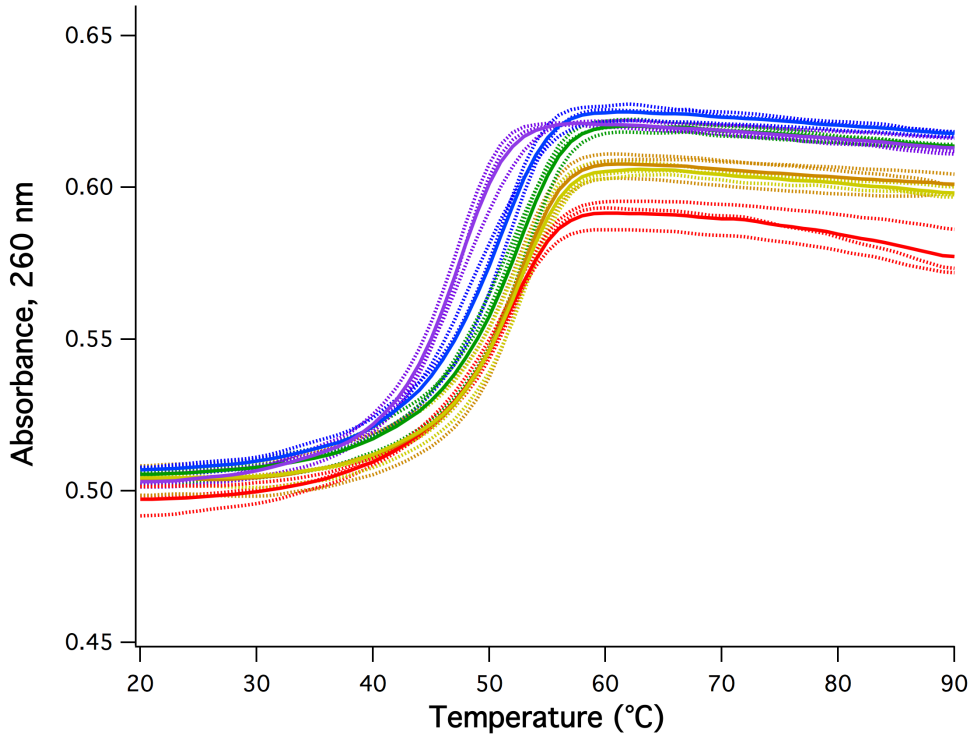

Figure 3.5 Melting traces of 32-mer DNA duplex (250 μg/mL) in 80% mol eutectic

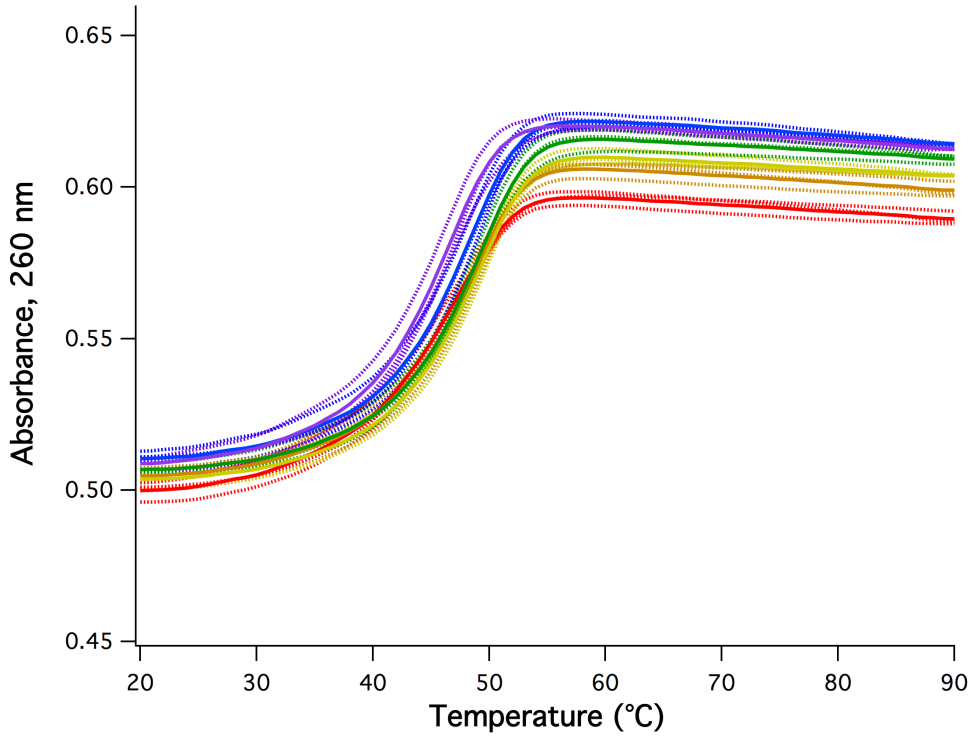

Figure 3.6 Melting traces of 32-mer DNA duplex (250 μg/mL) in 90% mol eutectic

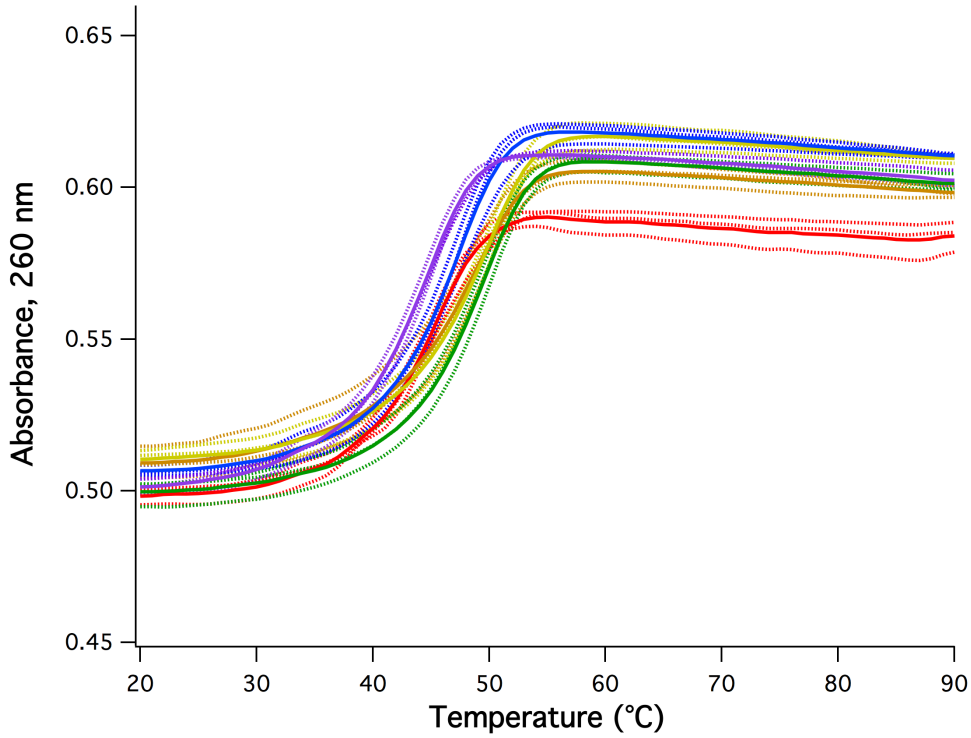

Figure 3.7 Melting traces of 32-mer DNA duplex (250 μg/mL) in 93% mol eutectic

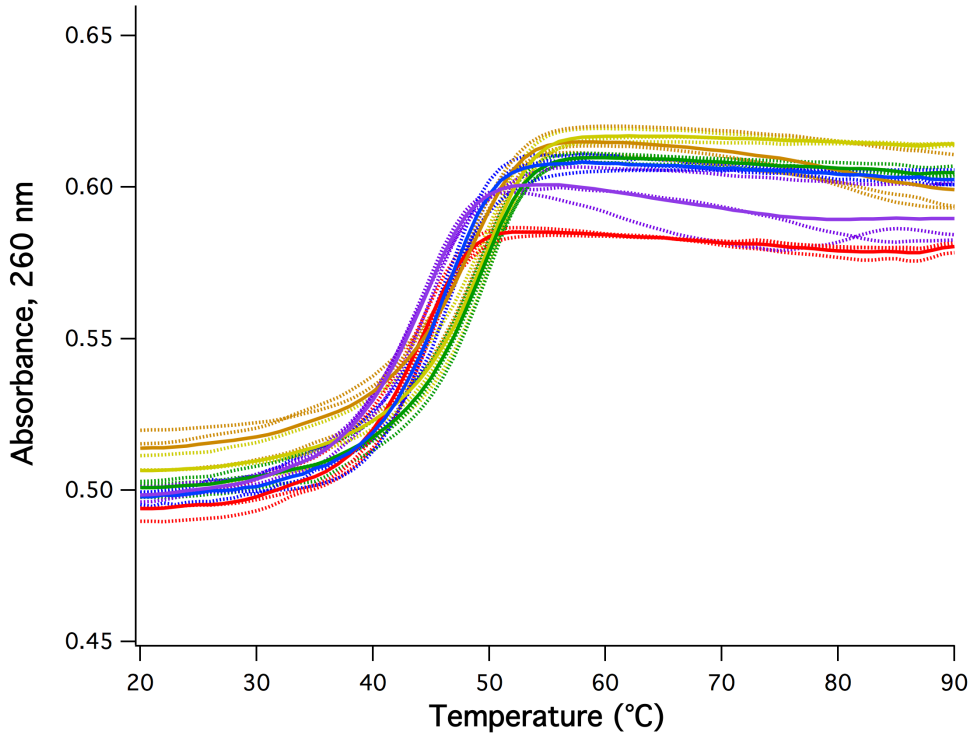

Figure 3.8 Melting traces of 32-mer DNA duplex (250 μg/mL) in 97% mol eutectic

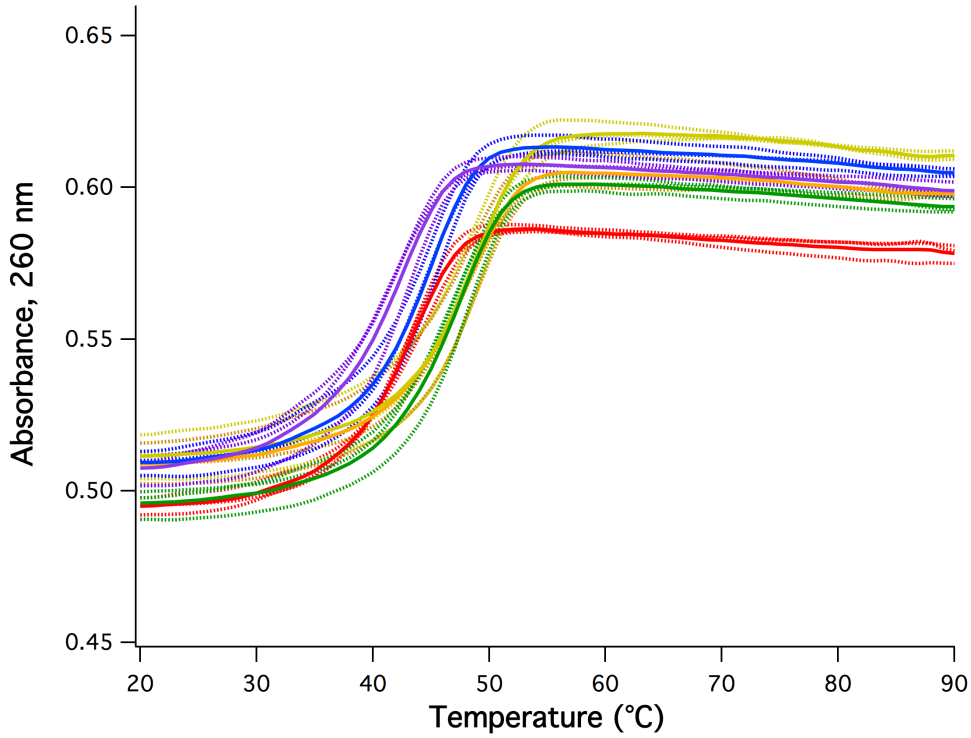

Figure 3.9 Melting traces of 32-mer DNA duplex (250 μg/mL) in 100% mol eutectic

As can be seen in Figures 3.1 to 3.9, all eutectic concentrations and glycerol : choline chloride ratios explored proved to have stable DNA secondary structure as indicated by cooperative, reversible melting transitions. As we aimed to have kinetic duplex annealing studies carried out at 20 °C, the lowest melting temperatures being roughly on the order of 40 °C in the allows us to fully utilize the eutectic parameter space for further experimentation without the need to factor in the equilibrium between duplex and single stranded DNA due to a mixed population of the two at a given temperature.

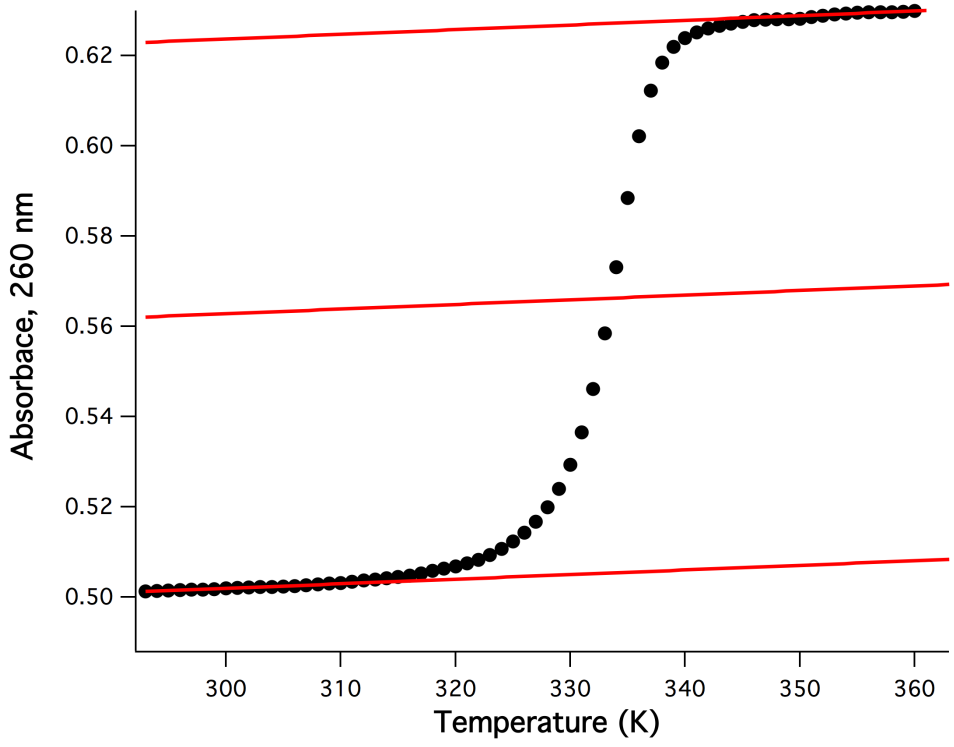

Figure 3.10 Melting curve 32-mer DNA in 20 mM sodium phosphate buffer, pH 7. DNA concentration was of 12.36 µM in strand. Upper and lower baselines applied to melting curve and a median line fit between them. The crossing point between the median line and the data is designated as the melting point.

In order to determine the melting temperatures from the data, a baseline correction method was utilized, as sloped baselines are clearly observed in the more concentrated eutectics. A popular method of determining T_m is to simply take the first derivative of the melting curve, and mark the point of the greatest slope as the melting temperature. However, this can often lead to overestimation of the T_m.[16] To accomplish this, baselines are applied to the upper and lower regions of the graph, corresponding to the single stranded and double stranded states respectively. A median line between the two baselines was plotted, and the point at which the median crosses the melting curve is determined to be the melting temperature[16]. Figure 3.10 shows an example of the method of T_m determination.

Table 3.1 T_m values of 32-mer DNA duplex, 250 µg/mL, in varying eutectic condition and dilutions. All solvents contain 20 mM sodium phosphate buffer, pH 7

	Glycerol : Choline Mol Ratio		
T_m (°C)	1 : 0.80	1 : 0.65	1 : 0.50
5% Eutectic	77.9±1	77.2±1	75.4±1
20% Eutectic	71.8±2	70.7±2	69.9±1
50% Eutectic	57.7±1	58.5±1	58.5±1
65% Eutectic	51.4±1	52.7±1	52.6±1
80% Eutectic	46.5±1	49.4±1	50.9±1
90% Eutectic	45.2±1	46.9±1	47.6±1
93% Eutectic	43.5±1	46.0±1	48.1±1
97% Eutectic	43.3±1	45.4±1	47.7±1
100% Eutectic	41.4±1	44.0±1	46.3±1

T_m (°C)	1 : 0.35	1 : 0.20	1 : 0.05

5% Eutectic	76.3±1	73.1±1	66.0±1
20% Eutectic	68.6±1	65.5±1	60.7±1
50% Eutectic	56.6±1	55.9±1	52.4±1
65% Eutectic	51.8±1	50.7±1	50.9±1
80% Eutectic	51.3±1	51.2±1	50.6±1
90% Eutectic	47.4±1	46.8±1	45.3±1
93% Eutectic	48.4±1	47.1±1	44.4±1
97% Eutectic	48.1±1	47.6±1	43.4±1
100% Eutectic	48.0±1	47.2±1	42.5±1

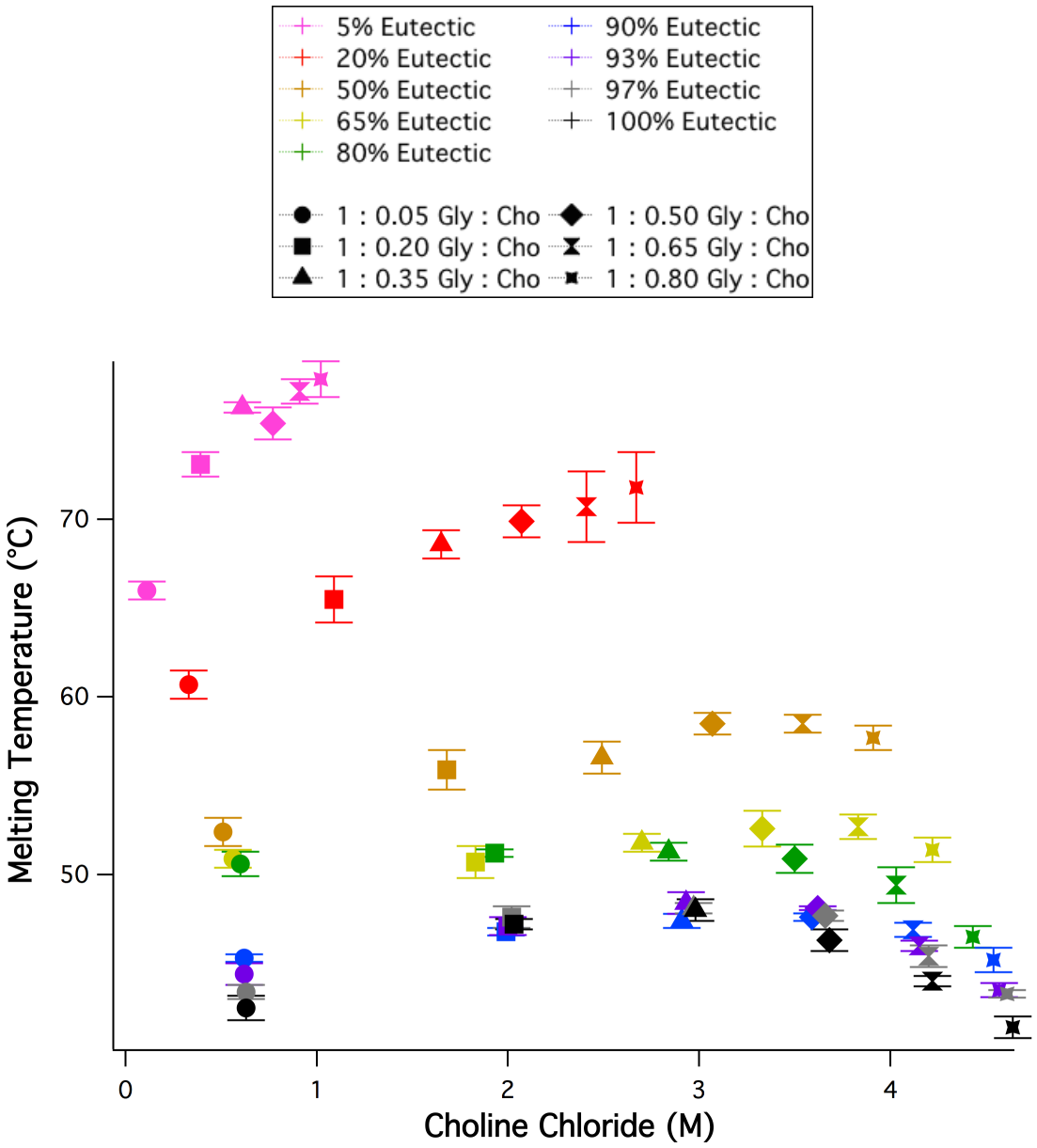

Figure 3.11 T_m values of 32-mer DNA duplex plotted as a function of choline chloride concentration in eutectic aqueous mixtures

A common trend can be seen through the set of samples of the 1:0.05 eutectic having the lowest hyperchromic effect. In addition to this, the hyperchromic effect decreases as total eutectic concentration increases, from a 16% increase in

absorbance at 260 nm in the 100% 1:0.05 eutectic, to a 25% increase in the 5% eutectics. The glycerol melts displayed an increase in hyperchromic effect of at most 14% when reaching the 65% by mol concentration that is of sufficiently high viscosity to observe kinetic effects in subsequent work in this study, with it decreasing further at higher glycerol concentrations. In buffer conditions, hyperchromicity is typically at a minimum of a 15% increase.[16] However, the solvent/exposed base interaction is likely to be different in the eutectics than in buffer, and despite this lower hyperchromicity, the glycerol curves still showed reversible transitions, with significant hysteresis that is supportive of a kinetic slowing of the reannealing process. Further work in exploring their utilization would absolutely be warranted. See Appendix for glycerol melt data.

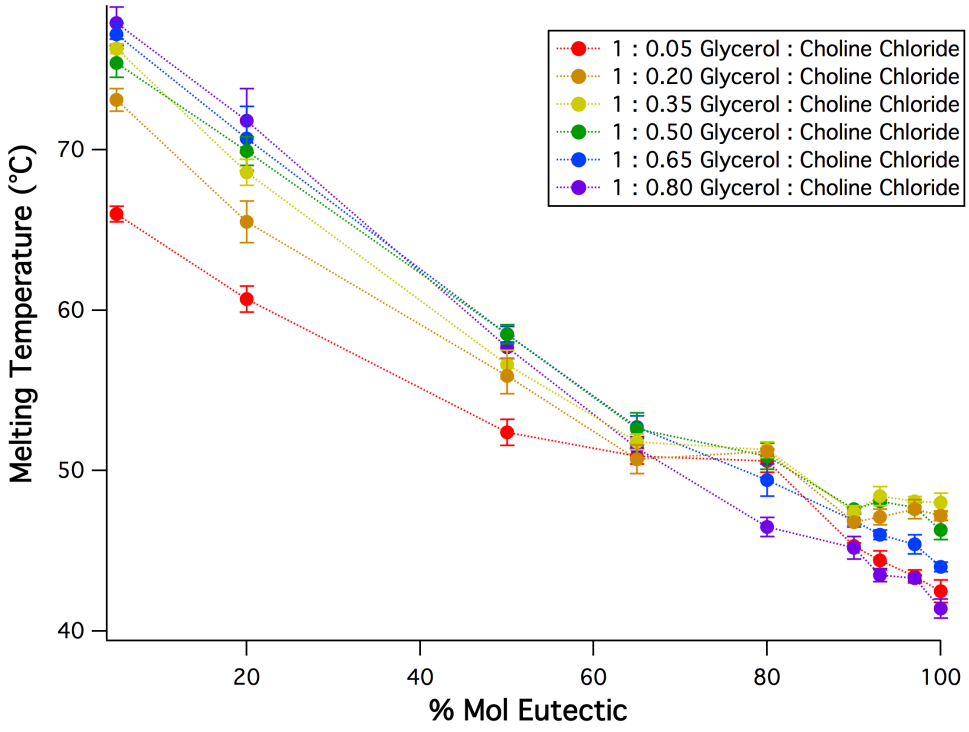

Figure 3.12 T_m of 32-mer as a function of mol percent eutectic diluted with water

3.3.2 Oligonucleotide Melts in Choline Buffer and Hairpin Melts in Eutectic and Buffer

In order to investigate if the high salt concentration is possibly responsible for any observed kinetic/thermodynamic effects in the following studies, melting temperatures in a range of buffered solutions with choline chloride present in similar concentrations to those present in the eutectic solvents were also obtained, as these solvents would also be investigated in the kinetic studies. Curves are shown in Figure 3.14, and associated melting temperatures in Table 3.2.

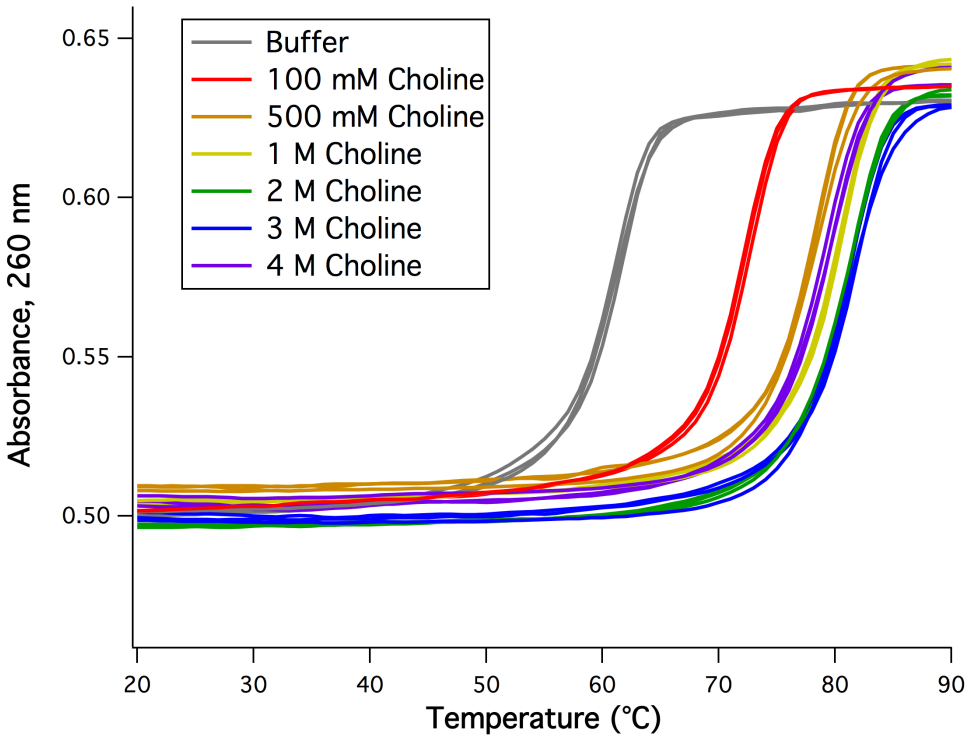

Figure 3.13 32-mer (250 µg/mL) in 20 mM sodium phosphate pH 7 buffer with varying choline chloride concentration

Given our hypothesis of large strands with self-complementarity

preferentially forming in viscous environments over a bimolecular structure, a unimolecular self-complementary DNA structure was also prepared for use in kinetic studies and stability within a eutectic observed, as seen in Figure 3.11.

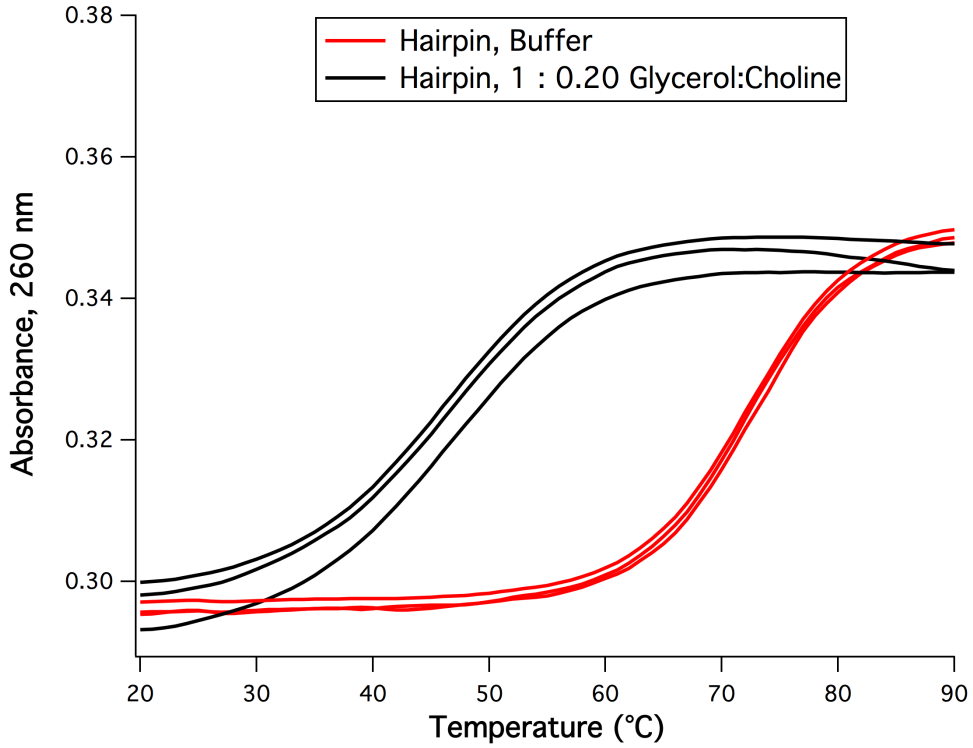

Figure 3.14 HP18 hairpin DNA (940 µg/mL) in 100% mol eutectic and 20mM pH 7 sodium phosphate buffer

Table 3.2 T_ms (°C) of 32-mer, 250 µg/mL, in aqueous buffer with varying choline chloride concentration, and T_ms (°C) of HP18, 940 µg/mL, in either aqueous buffer or a eutectic. All solvents contain 20 mM pH 7 sodium phosphate buffer.

Non-Eutectics	**T_m (°C)**
32-mer Duplex - 0 M Choline Chloride	60.5±0.4
32-mer Duplex - 100 mM Choline Chloride	71.7±0.3
32-mer Duplex - 500 mM Choline Chloride	77.6±0.1
32-mer Duplex - 1 M Choline Chloride	79.7±0.2
32-mer Duplex - 2 M Choline Chloride	80.4±0.2
32-mer Duplex - 3 M Choline Chloride	80.6±0.2
32-mer Duplex - 4 M Choline Chloride	78.6±0.4
HP18 – 0 M Choline Chloride	45.3±0.6
HP18 – 100%, 1 : 0.20 Eutectic	71.7±0.6

The hairpin also proved to have stable secondary structure under eutectic conditions at room temperature. Of note is the low increase in hyperchromicity at 16%, but this is not surprising given a large proportion of the strand is in a single stranded form within the loop of the hairpin. In addition, the hairpin melting temperature was determined through taking the derivative of the curve and marking the peak, as the more accurate baseline correction method could not be used due to the difficulty in determining a good baseline with the broad transitions in the eutectic and inability do discern an upper baseline in the buffer solution.

3.3.3 Thermodynamic Analysis of Melting Curves

Using the melting data obtained in the previous experimental work, thermodynamic parameters can be acquired. The data must first be converted to an equilibrium constant. This is accomplished by normalization of the melting data

with the baselines determined earlier in Figure X using the following equation:

$$f = (A_{ss} - A)/(A_{ss} - A_{ds})$$

With A_{ss} corresponding to the upper baseline, A the absorbance value at a given temperature, A_{ds} the lower baseline, and f the fraction in dsDNA form.

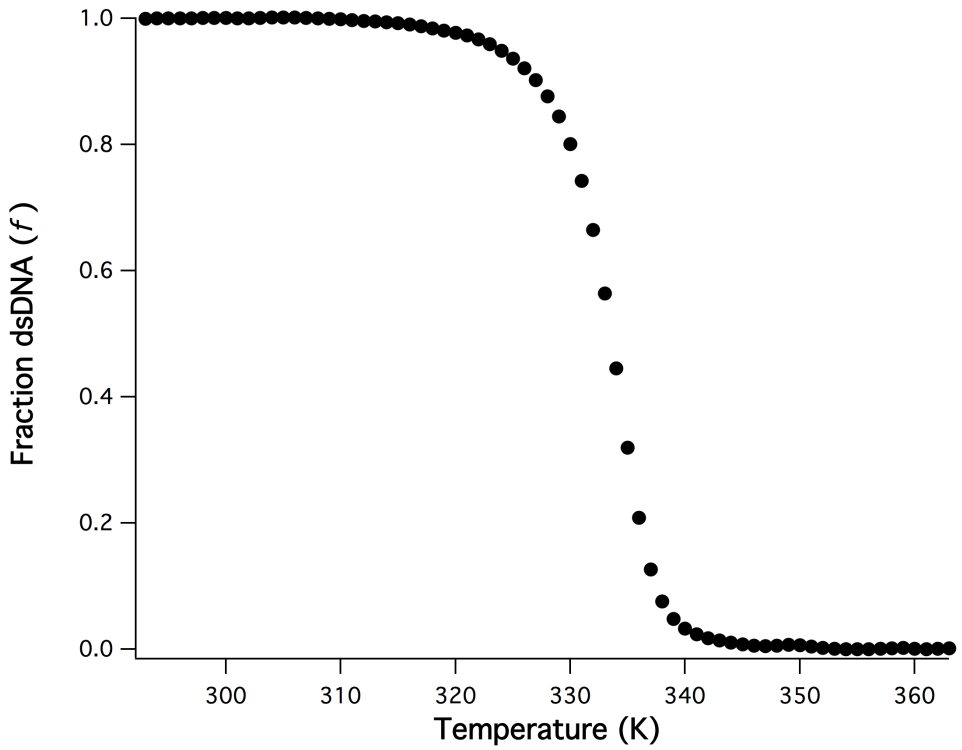

Figure 3.15 Conversion of melting data to fraction dsDNA data for analysis work using DNA in 20 mM sodium phosphate pH 7 buffer (melting data from Figure 3.10)

Once the fraction folded is obtained, it must be converted to an association constant. Given a bimolecular reaction of two complementary strands, the following equation is utilized:

$$K_a = \frac{f}{C_o(1-f)^2}$$

K_a is the association constant, f the fraction in dsDNA form, and C_o the initial strand concentration of the two complementary strands. This calculation is only done for values ranging from f = 0.85 to 0.15, in order to ensure the fitting is only done in the region in which the K_a will give a linear fit in the following Van't Hoff plot.[17]

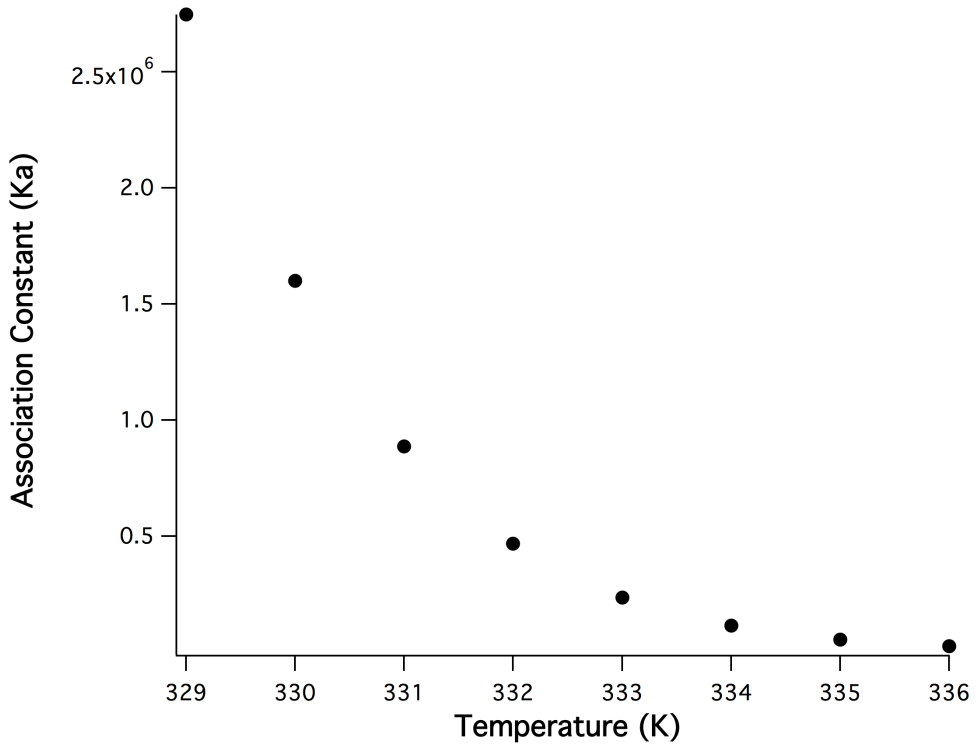

Figure 3.16 Conversion of fraction of dsDNA to association constant of the reaction, DNA in 20 mM sodium phosphate pH 7 buffer (melting data from Figure 3.10)

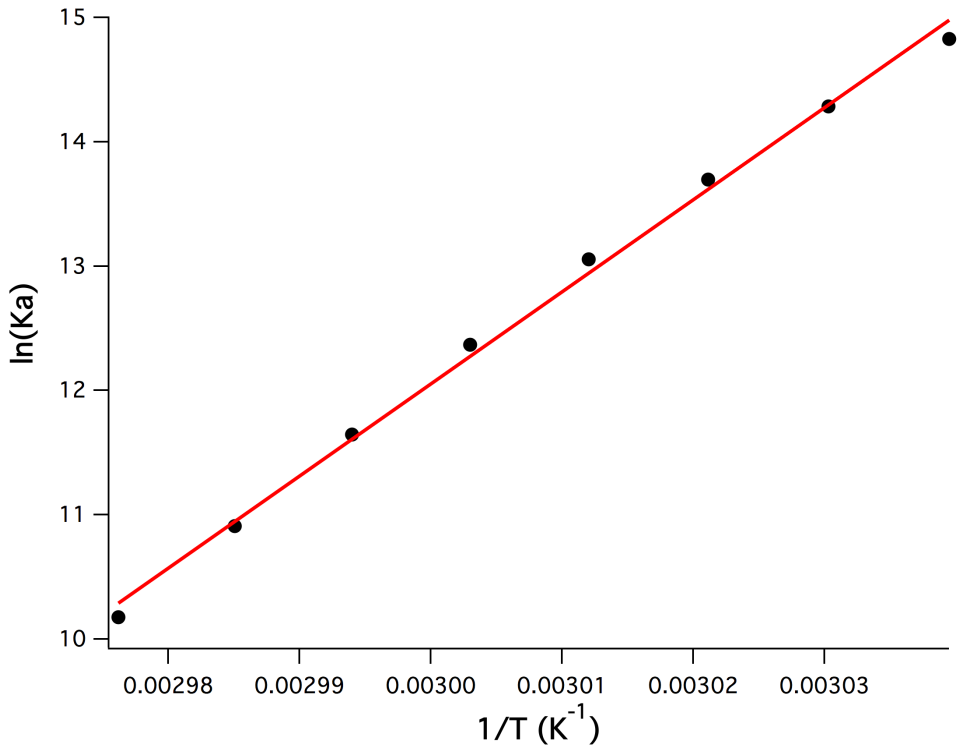

Figure 3.17 Van't Hoff plot for determination of enthalpy and entropy of the melting transition (melting data from Figure 3.10)

Once plotted as the natural log of the association constant as a function of inverse temperature, Figure 3.16 is obtained. The slope of the curve is equal to -ΔH°/R, with R being the gas constant. The intercept is equal to ΔS°/R. The values can be determined provided a linear fit of the melting data to the Van't Hoff plot, and from them the ΔG°. The parameters are listed below in Table 3.3 through Table 3.5, and displayed in Figure 3.17. Unsurprisingly it can be seen that the ΔG°s obtained throughout the eutectic conditions correlate fairly well with the stability as indicated by melting temperatures, as shown in Figure 3.11 and Figure 3.17.

Table 3.3 Enthalpy of melting transition

Glycerol : Choline Mol Ratio

-ΔH° (kcal/mol)	1 : 0.80	1 : 0.65	1 : 0.50
5% Eutectic	129±6.3	137.8±11.4	132.7±15.9
20% Eutectic	96.3±14.6	97.5±13.4	98.3±9.8
50% Eutectic	95.8±9.6	104.4±6.2	99.8±6.8
65% Eutectic	86.4±3.7	85.5±3.2	72.4±6.7
80% Eutectic	101.6±5.5	92.2±4.2	92.7±3.4
90% Eutectic	88.9±5.6	88.3±3.3	87.8±4.5
93% Eutectic	94.8±4.9	92.8±2.3	91.6±5.7
97% Eutectic	95.3±8.2	105.4±9.4	91.2±8.4
100% Eutectic	94.6±8.9	101.3±10.1	99.4±4.5

-ΔH° (kcal/mol)	1 : 0.35	1 : 0.20	1 : 0.05
5% Eutectic	135.2±1.2	118.9±15.9	134.3±14.3
20% Eutectic	99.4±18.9	97.8±23.3	104.5±28.5
50% Eutectic	90±8.6	89.9±10.8	92.2±5.9
65% Eutectic	77.5±4.5	71.3±11.2	103.4±9.5
80% Eutectic	96.7±10.9	101.7±8.0	84.0±9.8
90% Eutectic	84.3±2.6	81.1±3.4	74.5±5.1
93% Eutectic	93.2±1.6	79.3±6.6	101.8±9.3
97% Eutectic	89.1±6.0	95.7±4.1	114.4±3.8
100% Eutectic	48.0±0.6	47.2±0.3	42.5±0.7

Table 3.4 Entropy of melting transition

Glycerol : Choline Mol Ratio

-ΔS° (cal/J mol)	1 : 0.80	1 : 0.65	1 : 0.50
5% Eutectic	343.9±16.9	369.9±32.0	357.2±44.9
20% Eutectic	255.5±41.0	259.9±37.7	263.1±28.0
50% Eutectic	266.1±28.3	291.5±18.3	277.6±20.0
65% Eutectic	242.7±10.9	238.9±10.1	198.8±20.2
80% Eutectic	294.4±17.5	262.4±12.8	262.7±9.9
90% Eutectic	255.6±17	252.4±10.2	250.4±13.9
93% Eutectic	276.0±15.1	267.4±6.9	261.6±17.6
97% Eutectic	277.5±25.8	307.4±29.8	260.7±26.1
100% Eutectic	277.4±27.9	295.9±31.8	287.8±14.0

-ΔS° (cal/J mol)	1 : 0.35	1 : 0.20	1 : 0.05
5% Eutectic	363.5±3.7	320,0±45.6	372.6±41.7
20% Eutectic	267.5±55.1	265.1±67.8	289.4±84.5
50% Eutectic	249.5±25.5	250.0±32.0	259.8±18.1
65% Eutectic	214.9±13.5	196.8±34.3	295.5±28.8
80% Eutectic	274.5±33.3	290.1±24.6	235.9±30.0
90% Eutectic	239.6±8.2	229.9±10.6	210.4±16.0
93% Eutectic	265.9±5.8	224.3±20.3	297.2±29.7
97% Eutectic	254.0±18.4	274.5±12.8	337.8±12.0
100% Eutectic	285.7±21.4	275.6±28.1	303.1±21.6

Figure 3.5 Gibbs energy at 37 °C of melting transition

Glycerol : Choline Mol Ratio

$-\Delta G^{37}$ (kcal/mol)	1 : 0.80	1 : 0.65	1 : 0.50
5% Eutectic	22.3±1.0	23.1±1.5	21.9±2.0
20% Eutectic	17.0±1.9	16.9±1.8	16.7±1.1
50% Eutectic	13.3±0.8	14.0±0.5	13.8±0.6
65% Eutectic	11.2±0.3	11.4±0.2	10.8±0.4
80% Eutectic	10.4±0.2	10.9±0.3	11.3±0.3
90% Eutectic	9.6±0.4	10.0±0.2	10.2±0.2
93% Eutectic	9.3±0.2	9.9±0.2	10.5±0.3
97% Eutectic	9.2±0.2	10.1±0.2	10.4±0.3
100% Eutectic	8.6±0.2	9.6±0.3	10.2±0.2

$-\Delta G^{37}$ (kcal/mol)	1 : 0.35	1 : 0.20	1 : 0.05
5% Eutectic	22.5±0.2	19.7±1.7	18.8±1.4
20% Eutectic	16.4±1.8	15.6±2.3	14.8±23.
50% Eutectic	12.7±0.7	12.5±0.9	11.7±0.4
65% Eutectic	10.9±0.3	10.3±0.6	11.8±0.5
80% Eutectic	11.6±0.6	11.8±0.4	10.9±0.6
90% Eutectic	10.0±0.0	9.8±0.1	9.3±0.2
93% Eutectic	10.7±0.2	9.8±0.3	9.7±0.2
97% Eutectic	10.4±0.3	10.6±0.2	9.7±0.1
100% Eutectic	10.8±0.4	10.4±0.3	8.9±0.2

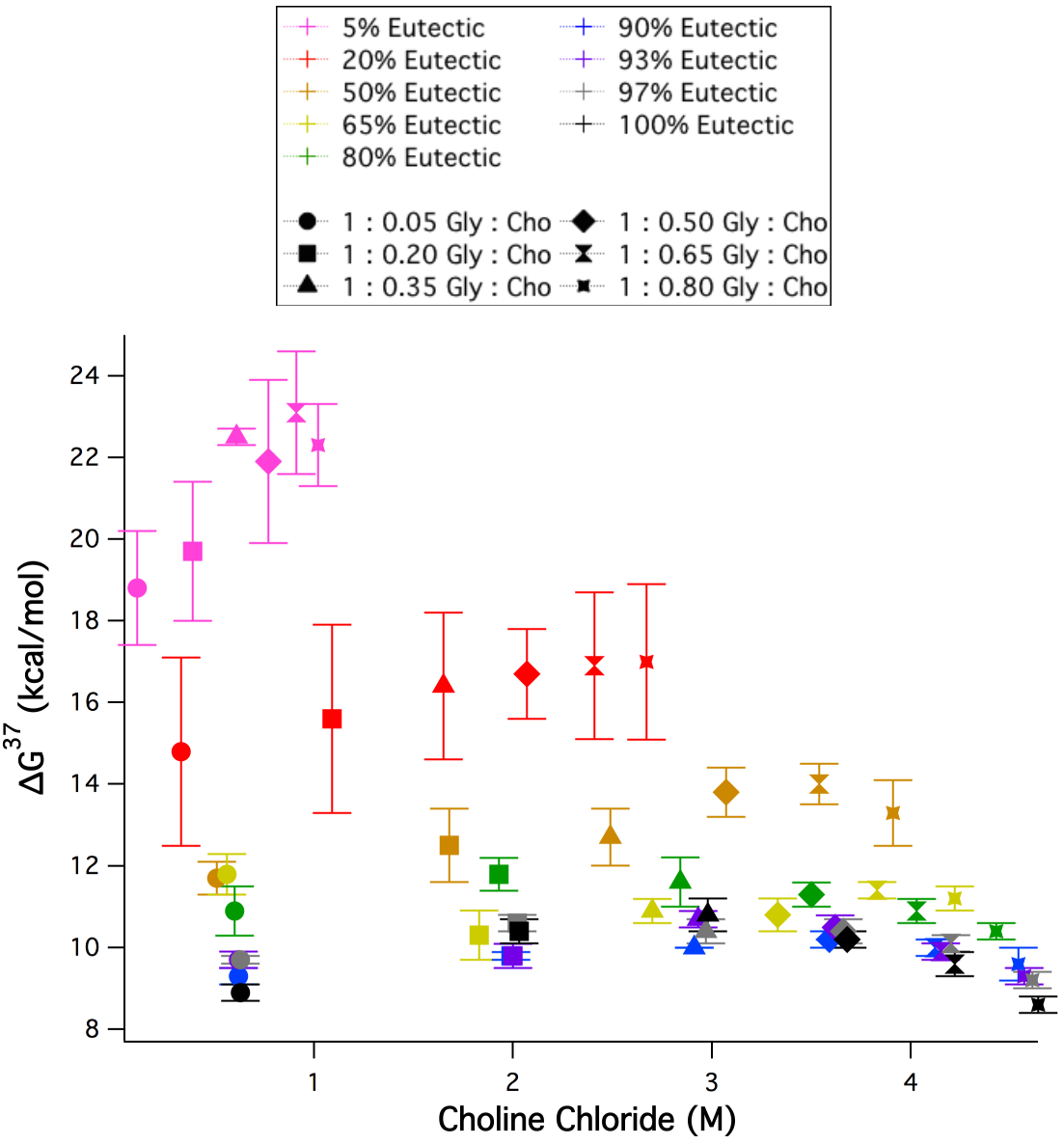

Figure 3.18 ΔG^{37} of 32-mer as a function of choline chloride concentration in eutectic aqueous mixtures

4 OLIGONUCLEOTIDE STRUCTURE IN EUTECTIC SOLVENTS

4.1 Introduction

In chapter three it was determined that stable secondary structure is maintained in the eutectic solvents. However, oligonucleotides can adopt a variety of secondary structural conformations while in their double stranded form. There are three major forms of nucleic acid structure, referred to as A-form, B-form, and Z-form[18]. Other types exist, such as C-form, which is similar in structure to B-form.

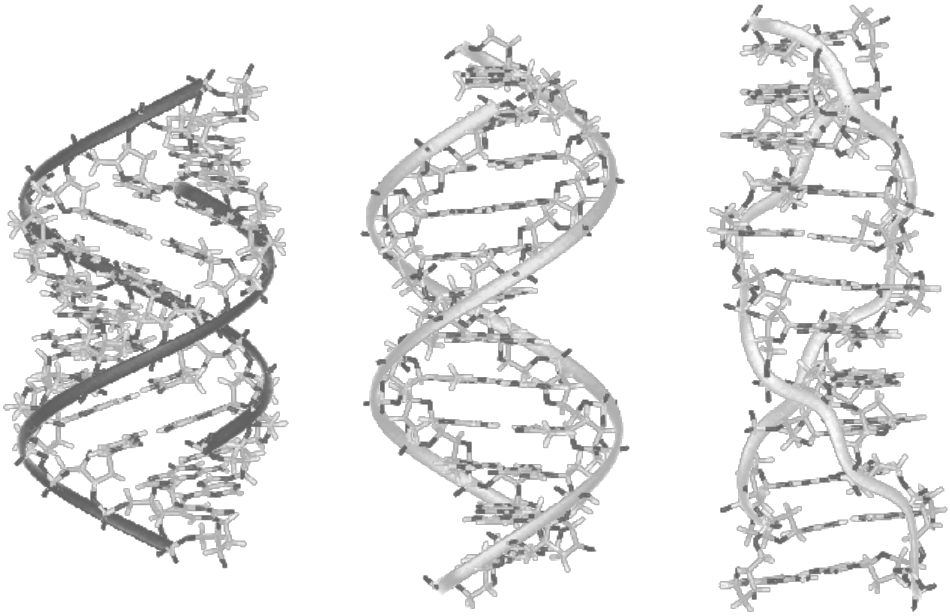

Common forms of DNA oligonucleotides, left to right, A-form, B-form, Z-form.

(Image obtained for use from public domain, http://commons.wikimedia.org/wiki/File:A-B-Z-DNA_Side_View.png, retrieved September 2014)

The form of secondary structure that DNA adopts is a result of the interaction

of these various features with environmental conditions . Given that this work is investigating the behavior of oligonucleotides in a non-standard environmental condition, it is important to establish what effects this environment is having on the structure. Typically, under hydrophobic, low water activity conditions, DNA adopts an A-form structure[19], but determination of the structure in a eutectic with low water activity and components of a more hydrophilic nature is necessary. Certain molecules can also cause DNA to adopt compacted forms, such as polyamines like spermidine[33], which may be of interest due to the high concentration of amines in the eutectic.

The structural properties of DNA in particular environments are an important consideration in as the field of DNA nanotechnology, which relies upon the specific parameters of B-form DNA.[30] Enzymes can also bind specifically to a particular form of DNA,[31] which would be of interest in studies involving enzymatic activity in eutectics.[34]

As the secondary structure of hybridized DNA cannot be determined from the UV-vis spectrum alone, circular dichroism spectroscopy (CD) is instead utilized. CD is used over a similar range of wavelengths as standard UV-vis studies of nucleotides. The method functions by observing the differences in absorbance between light that has been circularly polarized to the right and light circularly polarized to the left in chiral molecules, such as the chiral centers seen in DNA.[35] Each form of DNA will absorb the light in a different fashion, allowing determination of structure type from the overall spectra. While fine detail of a structure can be

difficult to discern from a CD-spectra, the overall secondary structure of the oligonucleotide can be established.

Some of the eutectics in the literature absorb strongly in the 260 nm region used in standard UV-vis studies, namely those with urea. While not an issue with the current eutectic composition, CD spectroscopy allows us to circumvent this issue in any future eutectics that include such molecules. However, any chiral eutectic components may pose issues in CD studies if they also strongly absorb over the same wavelengths that DNA does.

4.2 Materials and Methods

4.2.1 DNA Preparation

DNA was prepared as described in 3.2.1.

4.2.2 Sample Preparation

Samples were prepared as described in 3.2.2. 5% Eutectics were not further pursued due to indiscernible viscosity difference to that of water.

4.2.3 Structural Studies

A Jasco J-815 CD spectrophotomer was used to attain the circular dichroism spectra. Measurements were taken at 20 °C and 85 °C for dsDNA and ssDNA signals respectively, from 350 nm to 220 nm at a scan speed of 200 nm/min and a bandwidth of 4 nm, averaged over three reads.

4.3 Results and Discussion

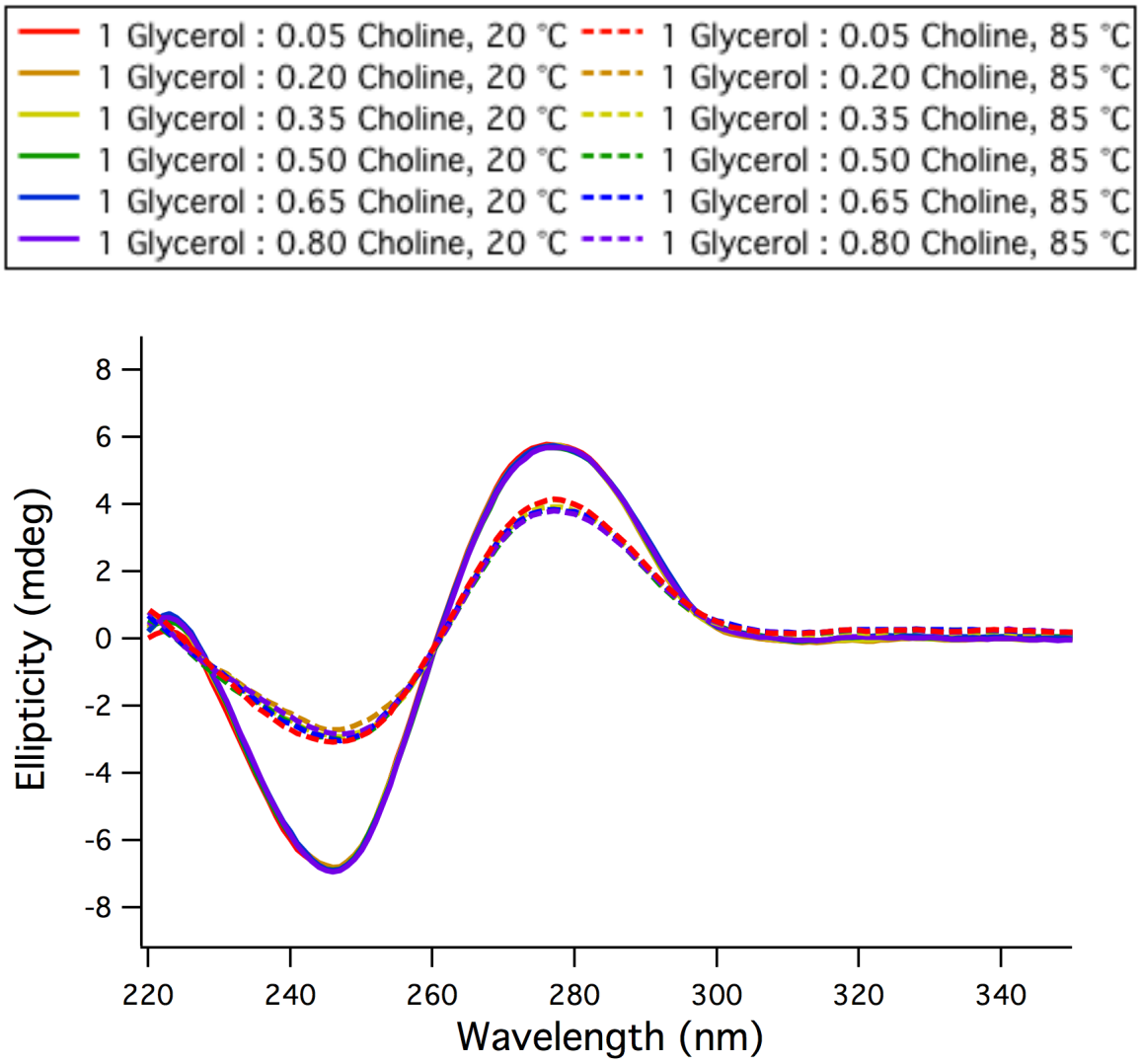

Figure 4.1 CD spectra of 32-mer DNA duplex (250 µg/mL) in 20% mol eutectic

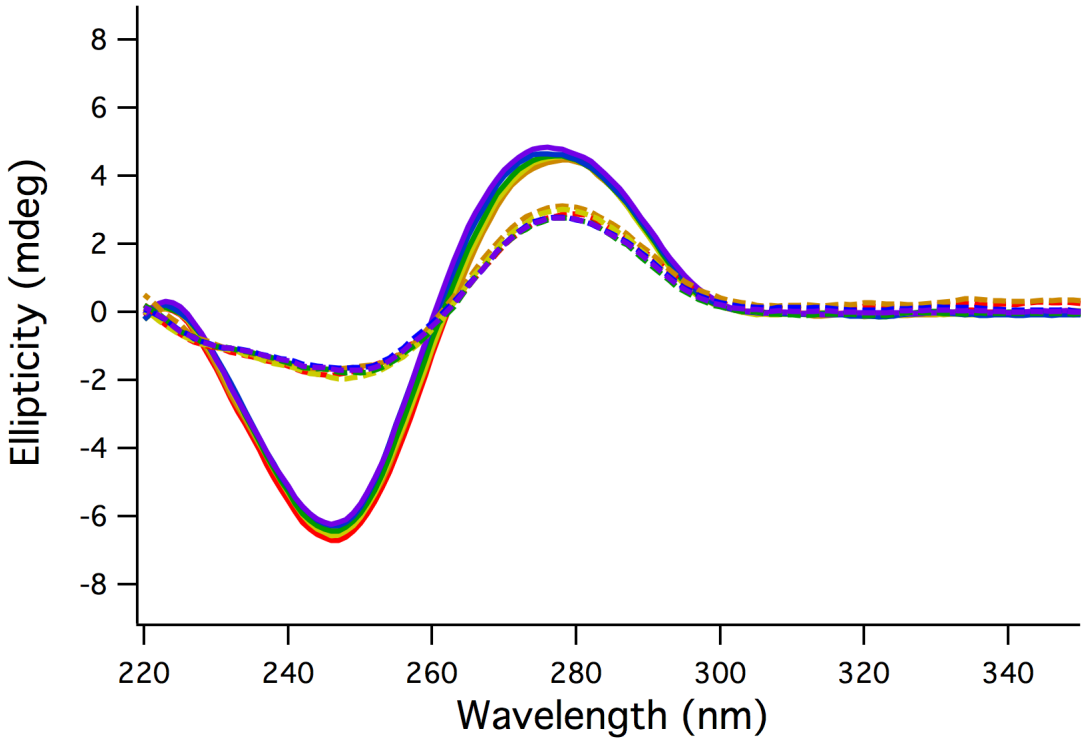

Figure 4.2 CD spectra of 32-mer DNA duplex (250 µg/mL) in 50% mol eutectic

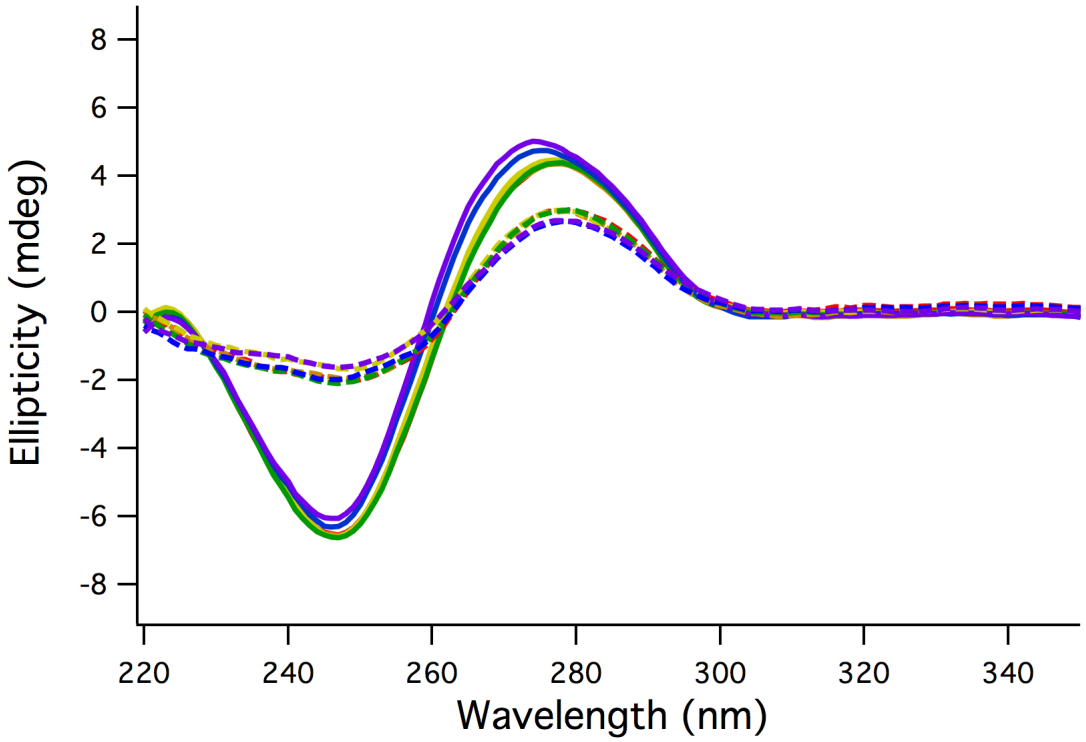

Figure 4.3 CD spectra of 32-mer DNA duplex (250 µg/mL) in 65% mol eutectic

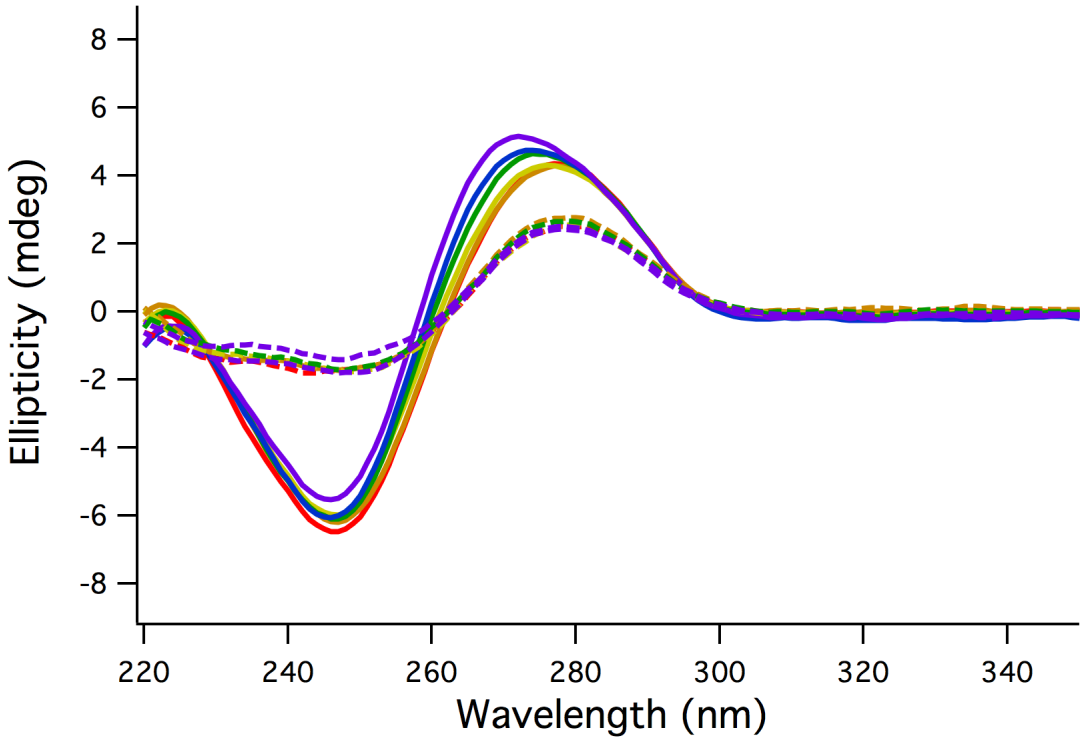

Figure 4.4 CD Spectra of 32-mer DNA duplex (250 µg/mL) in 80% mol eutectic

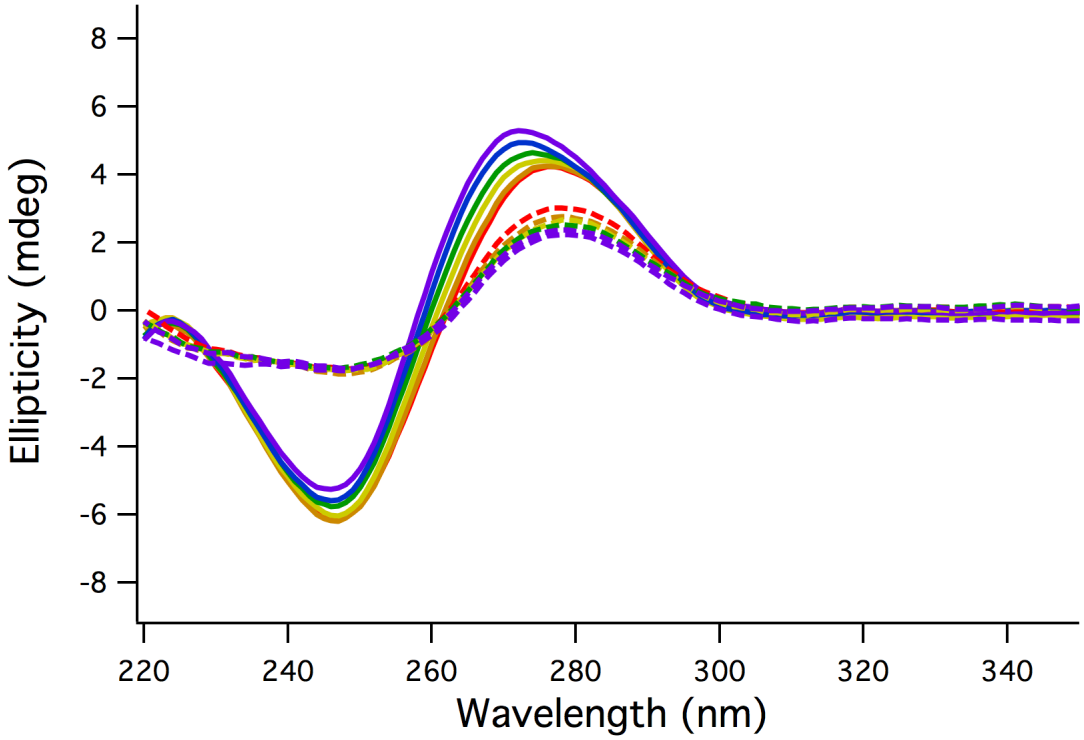

Figure 4.5 CD Spectra of 32-mer DNA duplex (250 µg/mL) in 90% mol eutectic

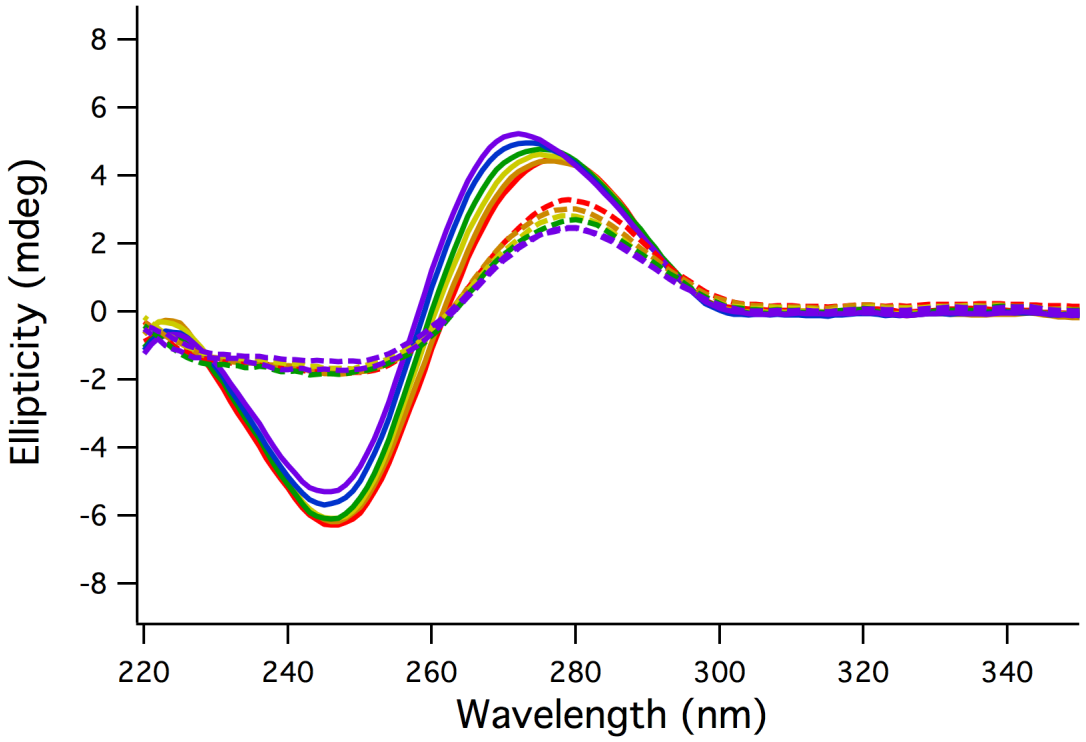

Figure 4.6 CD spectra of 32-mer DNA duplex (250 µg/mL) in 93% mol eutectic

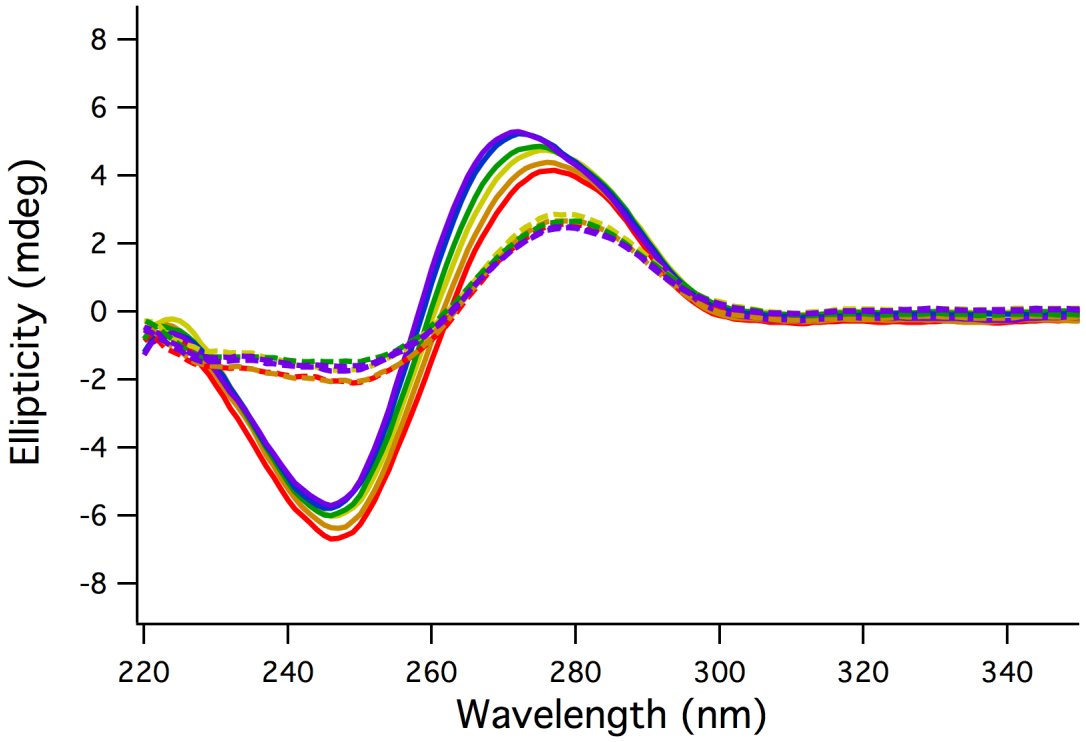

Figure 4.7 CD spectra of 32-mer DNA duplex (250 µg/mL) in 97% mol eutectic

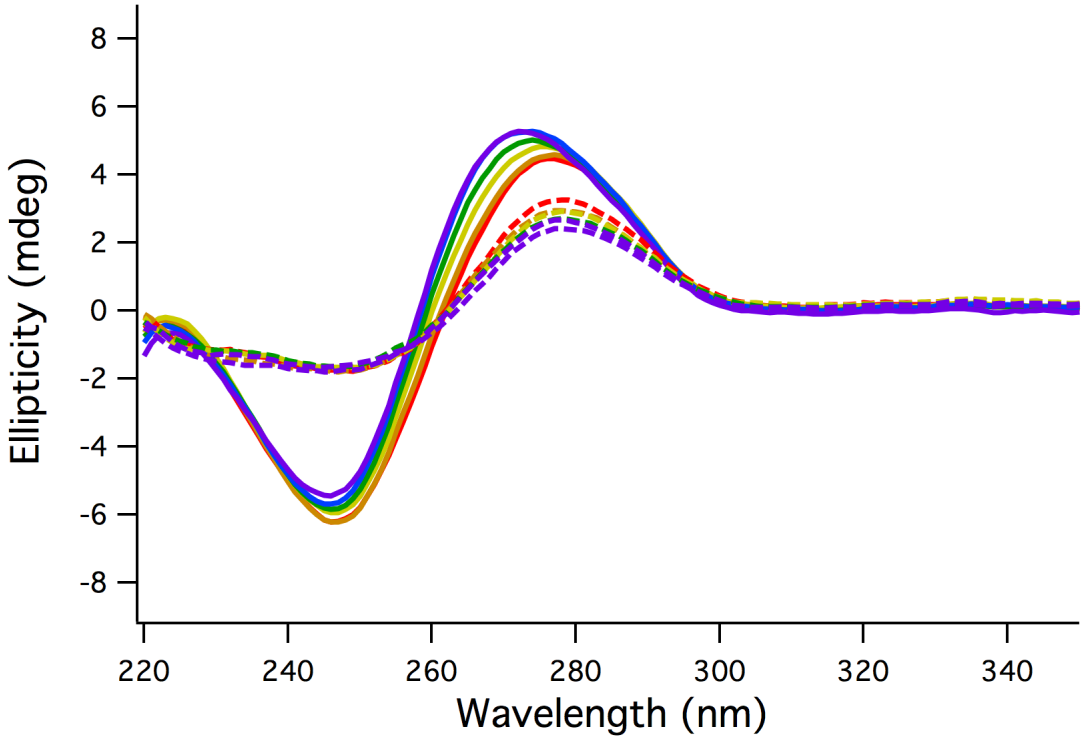

Figure 4.8 CD spectra of 32-mer DNA duplex (250 µg/mL) in 100% mol eutectic

We show here a mixed sequence oligonucleotide adopts a B-form structure for the entire range of explored glycerol : choline molar ratios, as well as the aqueous mixtures of these eutectics. The structure of the DNA begins showing a dependence on the choline concentration when 50% mol eutectic is present, with a blue shifting and intensity increase of the A_{280} peak, and a similar blue shifting and intensity decrease in the A_{245} peak, Figures 5-12. These changes are indicative of a small shift towards a more A-form like spectra as a function of increasing choline concentration[20]. It has been shown that choline binds preferentially to the minor groove of A-T sites and can trigger small changes in the structure of the minor groove[21].

C-form needs to be considered as another possible structure. An example of C-form from the literature[22] demonstrates that the structure undergoes a different transition as observed in their work, with C-form DNA losing most of the intensity of the 280 nm peak, indicating that the variants observed here are all predominantly structurally similar to B-form.

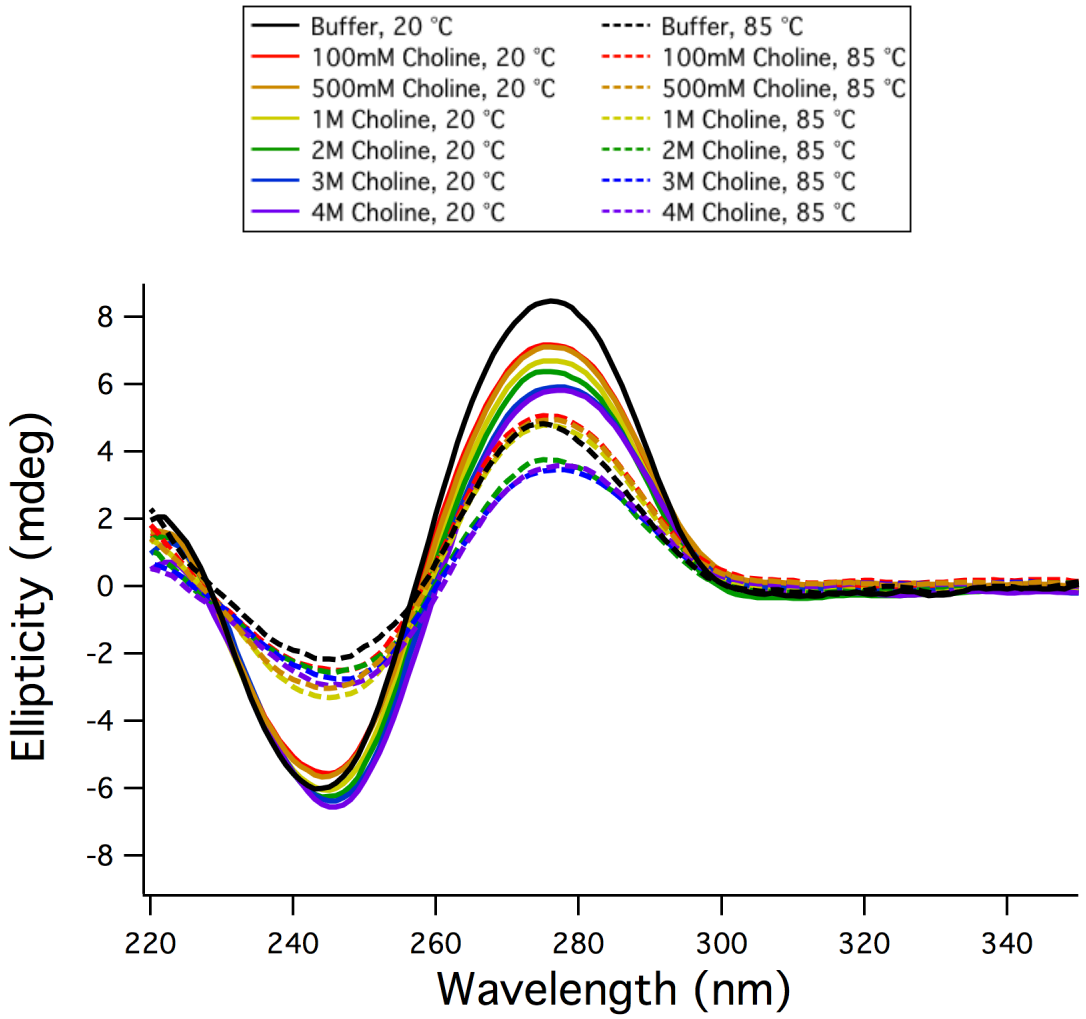

Figure 4.9 CD spectra of 32-mer DNA duplex with varying choline concentration in buffer

Choline in buffer solutions over a similar range of molarity as present in the

eutectics demonstrate a shifting as well, with additional choline shifting the spectra in the opposite direction as that of the eutectics in intensity, Figure 4.9, although with none of the blue or red shifting as seen in the eutectics. This indicates that choline concentration alone is not sufficient to induce the conformational changes observed in the eutectic to the oligonucleotide, but that the solvent environment as a whole must be considered, as it will influence the nature of the choline chloride and DNA interaction.

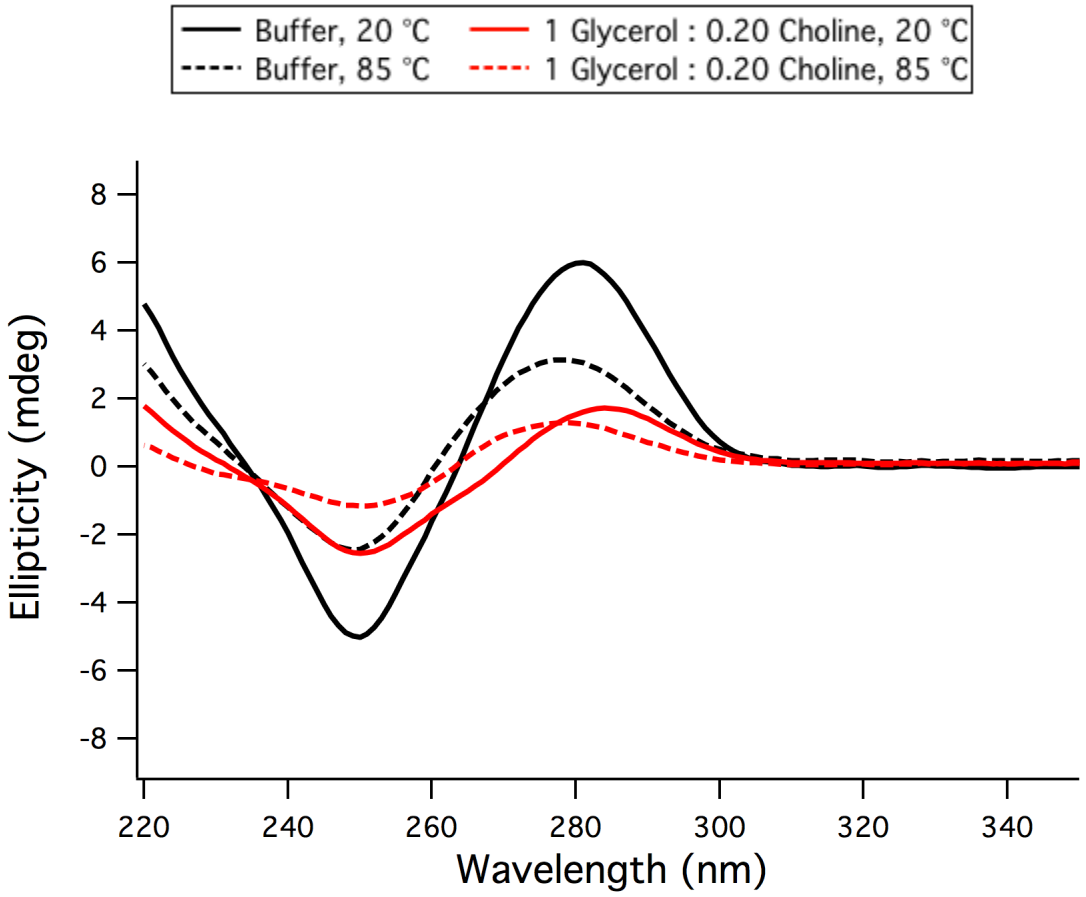

Figure 4.10 CD spectra of HP18 in either buffer or 1:0.20 glycerol:choline eutectic

HP18 was tested in 100% eutectic of 1:0.20 glycerol : choline as well, as seen in Figure 4.10. While a significant drop in signal intensity and a small red shifting of

the peaks is observed, a melting curve demonstrates a similar degree of hyperchromicity between the hairpin in buffer and in eutectic as seen in Figure 3.13, indicating a stable hairpin under both conditions. Of interest is also that the 270 nm peak in the eutectic at 85 °C has the same peak wavelength as that of the 85 °C in buffer, while at 20 °C there is a 3 nm red shift of the peak present in the spectra. This may be indicative of any interactions between the eutectic and the oligonucleotide being specific to the double stranded form.

5 KINETICS OF REANNEALING IN EUTECTIC SOLVENTS

5.1 Introduction

A key component of our study concerning reannealing of oligonucleotide strands in viscous solvents after thermal deannealing is the rate constant of the reannealing reaction. Rate constants of duplex formation for short oligonucleotides have been studied in the literature[32] and shown in numerous buffer conditions, and a large amount of work has been done in hybridization to immobilized DNA,[38][39] but the reannealing of complementary oligonucleotides in a eutectic solvent has yet to be explored.

Rate constants for oligonucleotide reannealing can be dependent on sequence length, sequence composition, and environmental conditions. A wide range of rate constants has been observed for different oligonucleotides, with a spread on the order from 10^2 to 10^7 M^{-1} s^{-1} [23]. It is therefore difficult to compare experimental results of one strand directly to another, as multiple factors can alter the rate constants between similar strands.

Alterations of rate constants can be accomplished through introduction of components such as mismatches, and even the AT and GC percentage composition will alter the rates[24], all of which can result in either a raising or lowering of the rate constant. Introduction of internal secondary structure such as hairpins will also change the rate constants[25].

We have aimed to reduce reannealing rates through environmental factors, which would keep the entire parameter space of DNA sequences available, rather

than limiting it to those which have a particular limiting property such as internal secondary structure or AT/GC tracks.

5.2 Materials and Methods

5.2.1 Sample Preparation

Samples were prepared as described in 3.2.1 and 3.2.2.

5.2.2 Determination of Quenching Time

1 mm quartz cuvettes were loaded with 250 μL of 100% 1:0.20 eutectic and the remaining volume filled with mineral oil. A thermocouple wire was inserted into the cuvette and the sample was heated to 85 °C. The sample was then plunged into an ice water bath and the temperature tracked over time.

5.2.3 Kinetics of Reannealing

Prior experimental work in determining association kinetics has been accomplished through either manual mixing or stopped flow experimental designs. The high viscosity of the solutions we have used make these methods difficult to employ, and so a premixed solution is employed and the kinetics monitored through recovery of an absorbance signal.

Samples were brought to 85 °C on a hot plate and plunged into ice water to reach 20 °C, then placed into the J-815 circular dichroism spectrophotometer to track over the course of twenty minutes at 245 nm, with reads being taken at one second intervals.

5.3 Results and Discussion

5.3.1 Determination of Optimal Thermal Quenching

The first experiment to conduct is to determine the proper thermal quenching time. Too much time spent cooling and reannealing data would be lost, but too little time and reannealing would not be observed at a constant temperature. Figure 5.1 below shows the temperature recorded by a thermocouple inside a cuvette being subjected to a plunge into ice water after heating to simulate the quenching of a sample of DNA containing eutectic. Using this data, a ten second quench was determined to be sufficient.

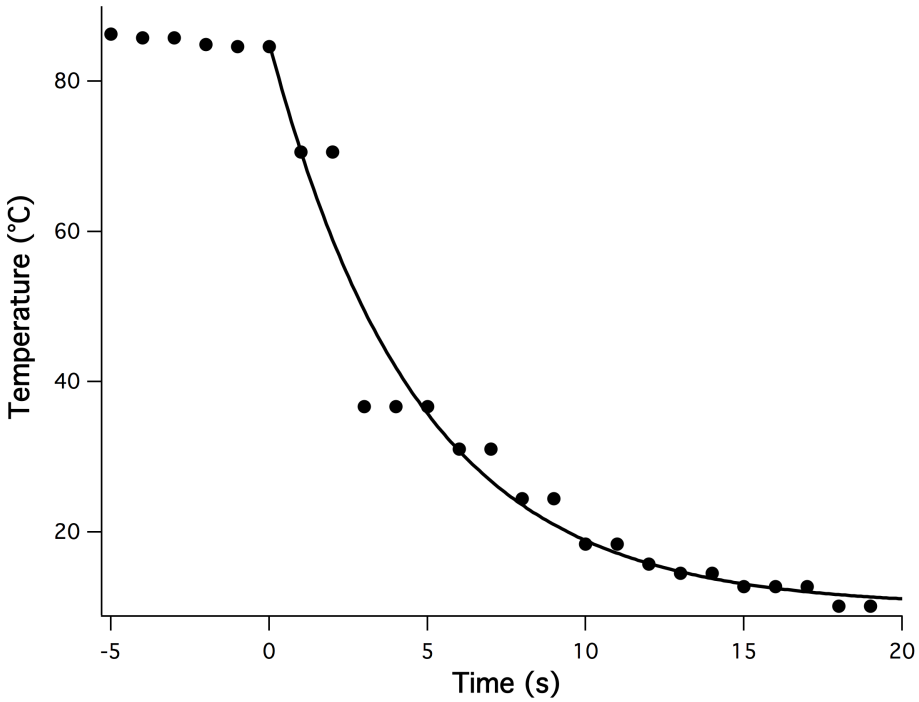

Figure 5.1 Quenching hot cuvette in ice water for determination of optimal quenching time

5.3.2 Reannealing Kinetics of Oligonucleotide in Eutectic Solvent and Aqueous Eutectic Mixtures

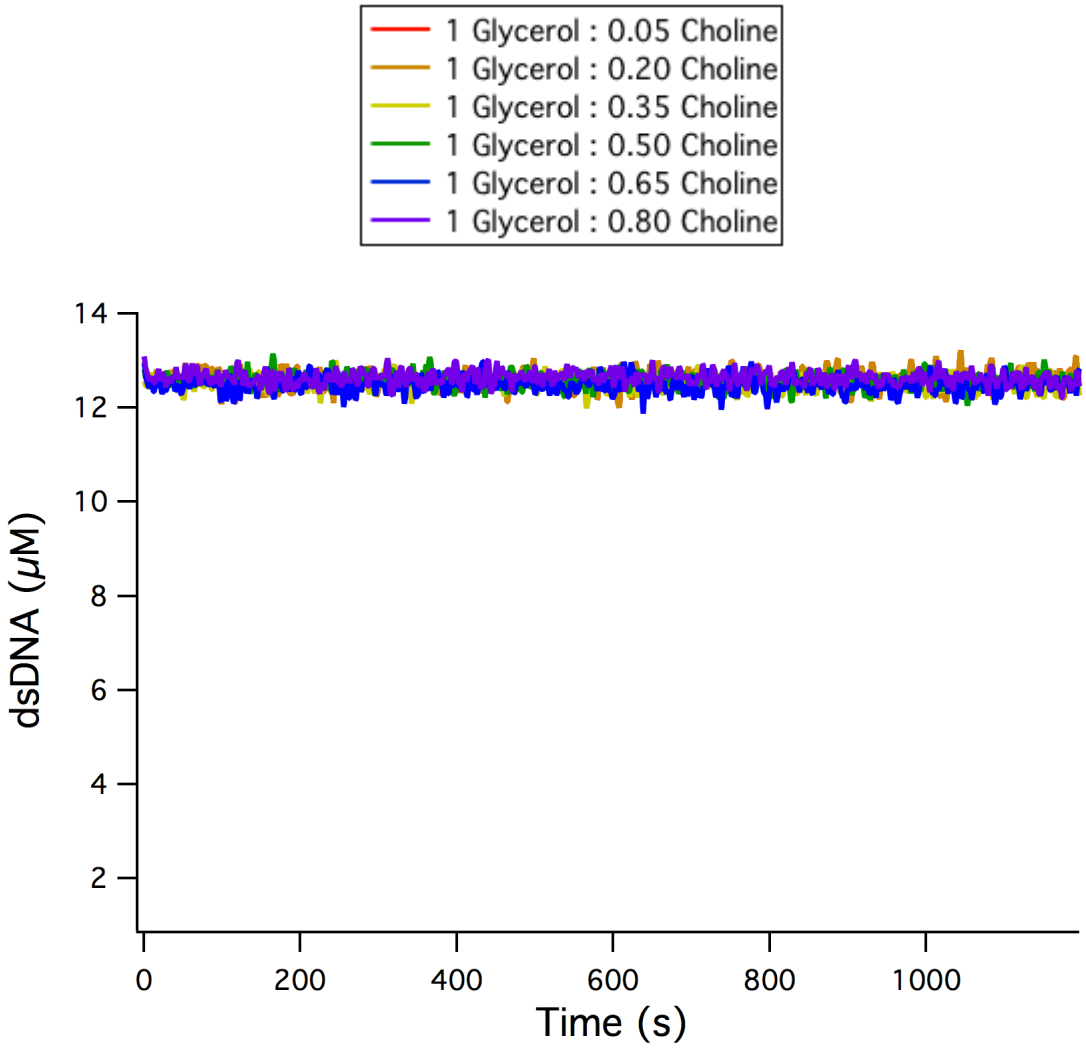

Figure 5.2 Recovery of hybridized 32-mer DNA duplex structure (250 μg/mL) in 20% mol eutectic

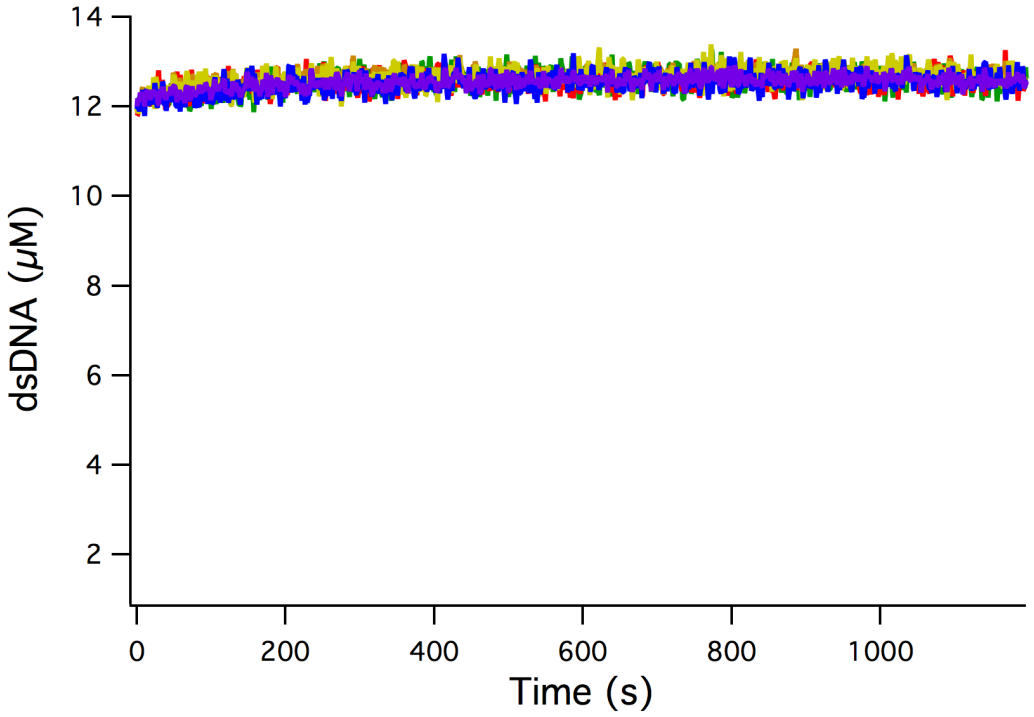

Figure 5.3 Recovery of hybridized 32-mer DNA duplex structure (250 μg/mL) in 50% mol eutectic

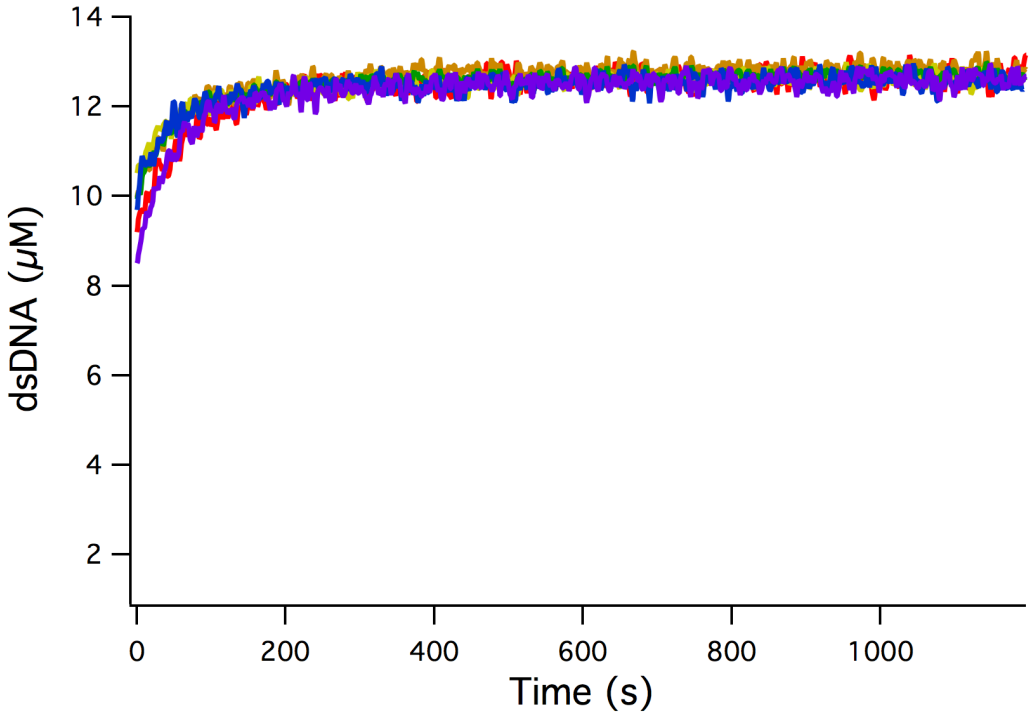

Figure 5.4 Recovery of hybridized 32-mer DNA duplex structure (250 μg/mL) in 65% mol eutectic

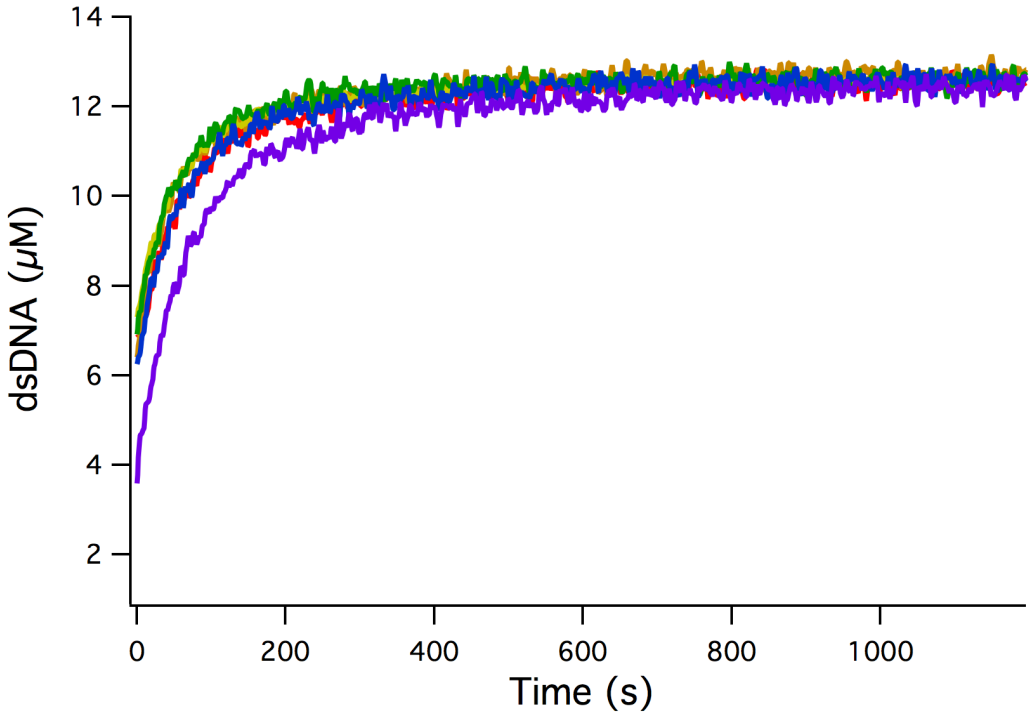

Figure 5.5 Recovery of hybridized 32-mer DNA duplex structure (250 μg/mL) in 80% mol eutectic

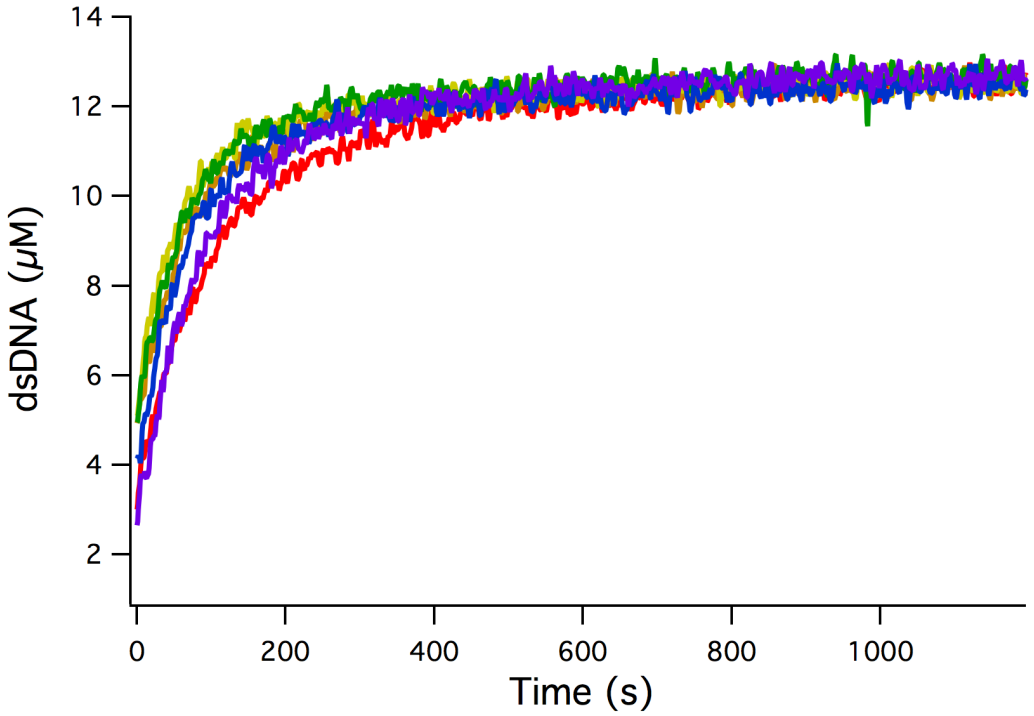

Figure 5.6 Recovery of hybridized 32-mer DNA duplex structure (250 μg/mL) in 90% mol eutectic

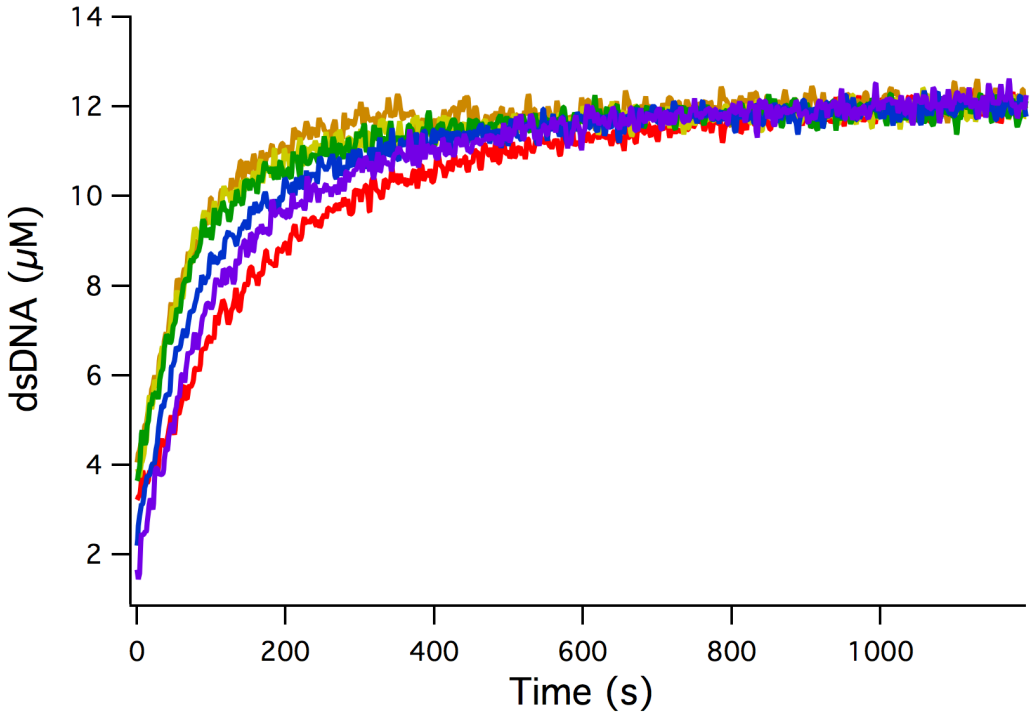

Figure 5.7 Recovery of hybridized 32-mer DNA duplex structure (250 μg/mL) in 93% mol eutectic

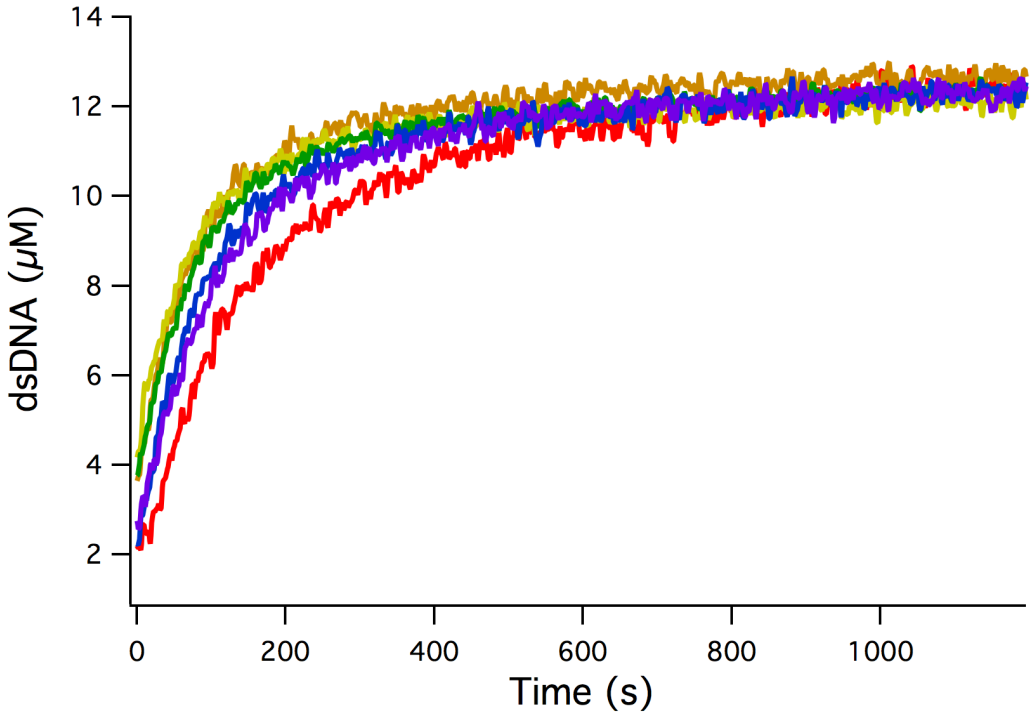

Figure 5.8 Recovery of hybridized 32-mer DNA duplex structure (250 μg/mL) in 97% mol eutectic

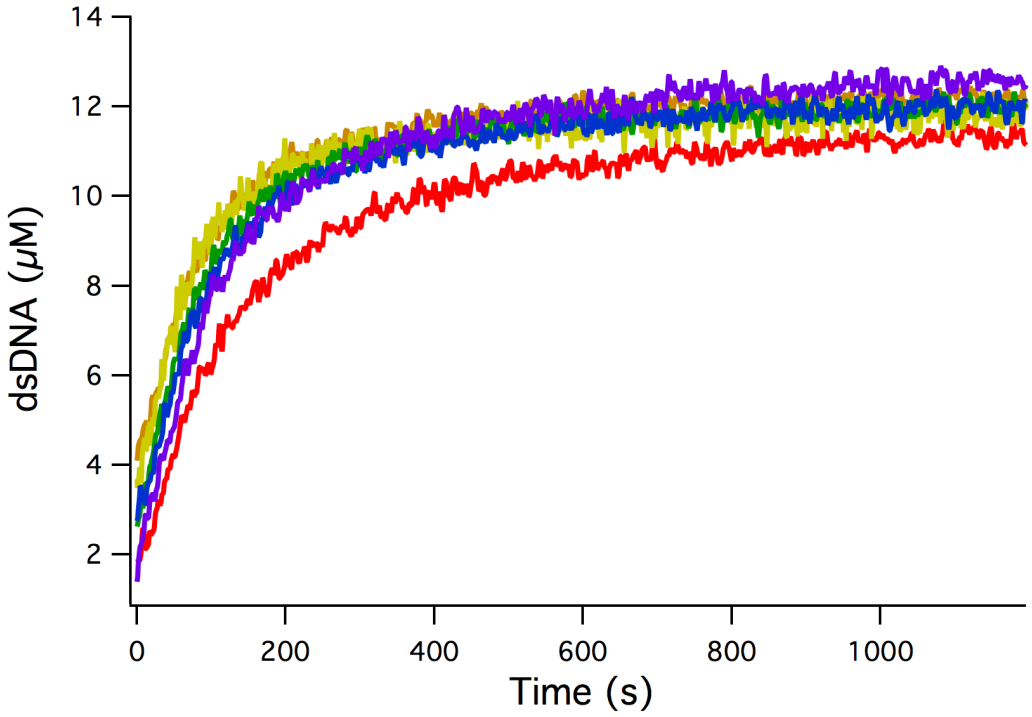

Figure 5.9 Recovery of hybridized 32-mer DNA duplex structure (250 μg/mL) in 100% mol eutectic

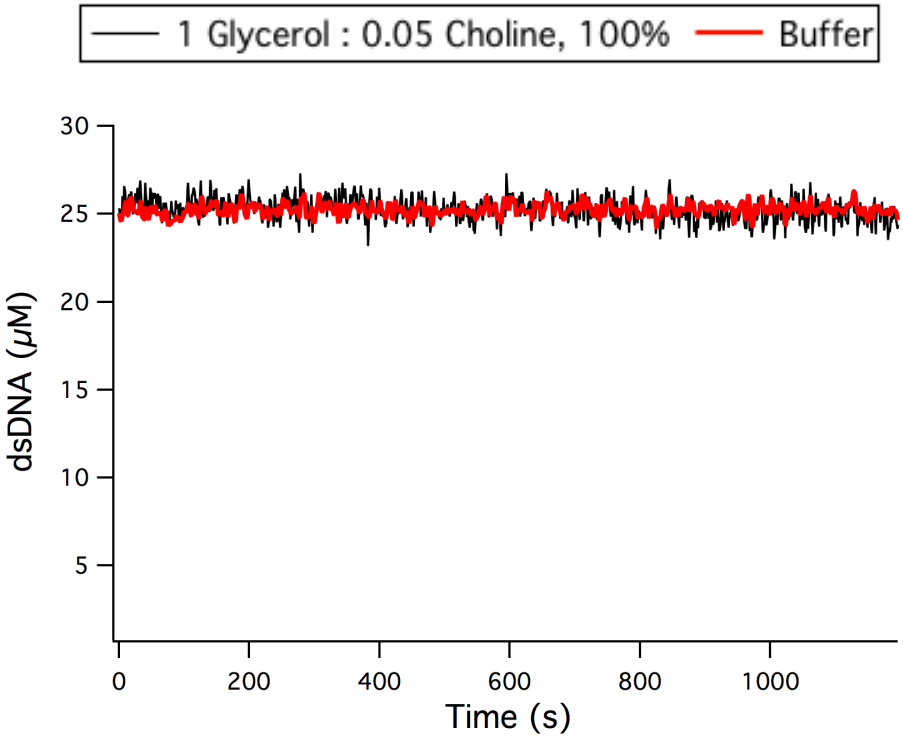

Figure 5.10 Recovery of HP18 DNA duplex structure in 100% mol eutectic and 20mM pH 7 sodium phosphate buffer

In order to monitor the reannealing process, the recovery of the dsDNA CD signal was observed after deannealing with heat and quick cooling to 20 °C in ice water. The signal at 245 nm was normalized between the ssDNA CD spectrum and the dsDNA CD spectrum for each sample and converted to μM of dsDNA present. In the less viscous solutions, the signal was seen to have completely recovered to the dsDNA intensity before the first read was obtained (t=15s), as seen in Figure 5.2. A small delay in the recovery is observed beginning with the 50% eutectic solutions, but fits are poor in this range. Once 65% eutectics are used, the delay is significant enough to achieve good fits using a second order kinetics equation, Figure 5.4 to Figure 5.9.

An increase in the total concentration of oligonucleotide was necessary in order to reach sufficient signal strength for the hairpin DNA, and so the concentration is double that of the 32-mer DNA. The hairpin, Figure 5.10, observed no delay in recovery of the dsDNA signal in either buffer or 100% mol eutectic, indicating that any reannealing process was completed before t = 15s. This indicates that the diffusive process is either the dominant effect of the reannealing under these conditions, or the unimolecular character of the hairpin allows for ease of the initial rearrangement and nucleation step and subsequent zipping.

The reannealing curves were fit to the following second order kinetics equation:

$$C_p = C_0 - \frac{1}{kt + \frac{1}{C_0}}$$

With C_p equal to the concentration of product, in this case dsDNA, and C_0 equal the initial concentration of one strand of ssDNA. *k* describes the rate constant for the equation of:

$$2A \xrightarrow{k} P$$

With A equal to ssDNA and P equal to dsDNA. The resulting rate constants are shown below in Figure 5.11 as a function of viscosity.

If we assume a purely diffusion controlled reannealing process, as is possibly suggested by the hairpin data in this experiment, then we can utilize a modified Stokes-Einstein equation to calculate the theoretical rate constant for the reannealing reaction in any of the solvents:

$$k = \frac{8k_bT}{3\eta}$$

However, rate constants using this estimation are vastly higher than those observed or seen in the literature[23] for similar oligonucleotide systems, demonstrating that a simple Stokes-Einstein model is not applicable here.

It can be observed that when comparing the rate constants in the eutectics to the viscosities, a linear relationship is not present. Each glycerol : choline ratio is fit with an exponential curve. Using this curve, we can calculate the theoretical

reannealing rate in a 1 cP solution of water, which give the range of rate constants seen in Table 5.1. When comparing the theoretical rate constants to that of each of the six 100% glycerol : choline ratio eutectics, a decrease in the rate constant ranging from two orders of magnitude in the most viscous 1 : 0.05 glycerol : choline ratio to an order of magnitude in the other, lower viscosity ratios is calculated.

It can also be seen that viscosity is not the only factor altering the reannealing rates, although it is necessary to observe the introduction of a delay in reannealing. Solutions of similar viscosity but with different concentrations of choline chloride can be seen to have a reduced rate constant as the amount of choline chloride increases, as seen in Figure 5.11.

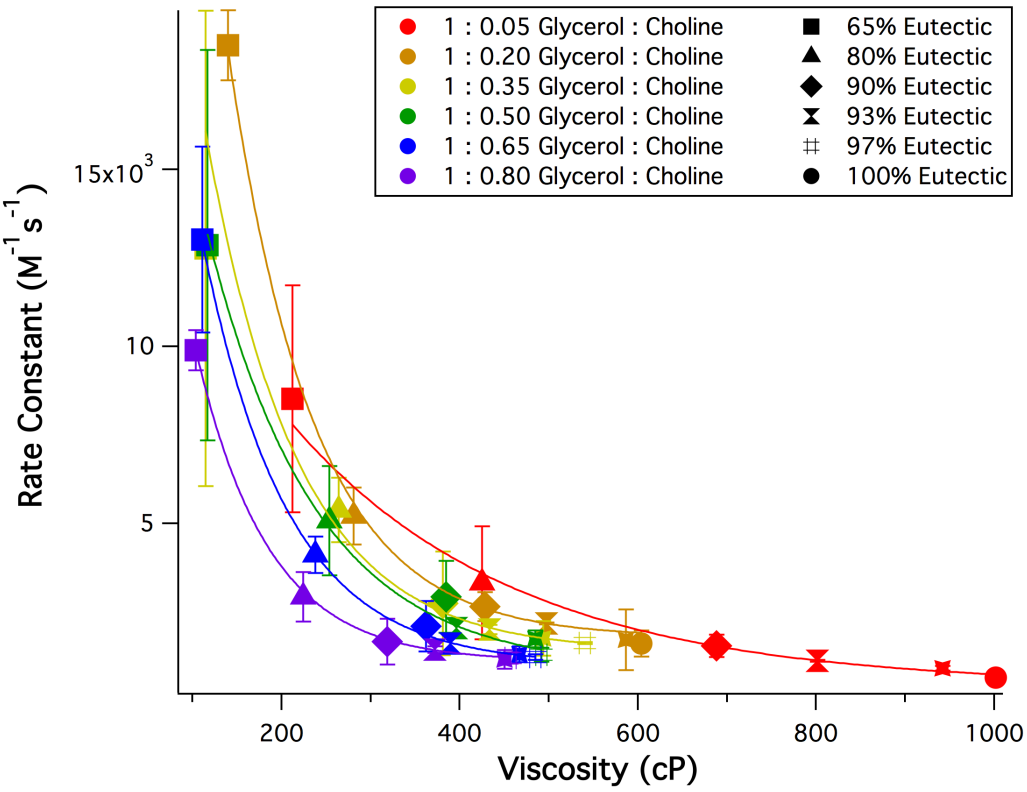

Figure 5.11 Rate constants of the reannealing of 32-mer oligonucleotides as a function of viscosity

Table 5.1 Rate constants of reannealing of a 32-mer, 250 µg/mL, in varying eutectic condition and dilutions. All solvents contain 20 mM pH 7 sodium phosphate buffer.

	Glycerol : Choline mol Ratio, Reannealing Rate Constants ($M^{-1}s^{-1}$)					
	1 : 0.80	1: 0.65	1: 0.50	1:0.35	1:0.20	1:0.05
Theoretical 1 cP	*3.1E4*	*3.8E4*	*3.2E4*	*4.4E4*	*7.1E4*	*1.7E4*
65% Eutectic	9.9E3	1.3E4	1.3E4	1.3E4	1.85E4	8.5E3
80% Eutectic	2.9E3	4.1E3	5.1E3	5.4E3	5.21E3	3.3E3
90% Eutectic	1.7E3	2.1E3	2.9E3	2.8E3	2.7E3	1.6E3
93% Eutectic	1.4E3	1.6E3	2.1E3	2.0E3	2.18E3	1.1E3
97% Eutectic	1.2E3	1.3E3	1.7E3	1.8E3	1.7E3	9.2E2
100% Eutectic	1.2E3	1.2E3	1.3E3	1.6E3	1.6E3	6.6E2
% Decrease from *1 Cp* to 100%	25.9x	31.0x	24.5x	27.2x	44.0x	26.0x

6 CONCLUSIONS

In this work we have demonstrated viable room temperature DNA oligonucleotide secondary structure over all investigated conditions of glycerol : choline chloride eutectic dilution and component ratios, ranging from a 1 : 0.05 molar ratio to a 1 : 0.80 molar ratio of glycerol to choline chloride as well as 5% by mol eutectic diluted with water to anhydrous 100% mol eutectic. A wider range of potential molar ratios observed when compared to previously reported work also highlights the need to more completely explore the parameter space available in eutectic compositions. Density and viscosity values of the range of eutectics have also been shown, and can be seen to rest within the range of values for water to glycerol. Of interest is the reannealing rate constants dependency upon not just viscosity, but also eutectic concentration and molar ratio, indicating that the identity of the solvent components can also possibly be altered to tune the rate constants if necessary. This better understanding of the parameter space available for eutectic composition can allow for such tunability to specific characteristics in future studies, be it the viscosity of the solvent or the stability of oligonucleotides.

We have found that nucleic acids exhibit a stable B-form structure over the entire range of solvent conditions, both anhydrous and hydrated, and the structure can be induced into making small changes through both modification of the glycerol : choline chloride molar ratio and dilution with water. The eutectics are further observed to modify the reannealing rate constants of DNA hybridization through

both viscosity and salt interactions, allowing for up to a two order of magnitude decrease in reannealing rates when compared to annealing under aqueous buffered conditions, or a theoretical decrease in the rate constant of annealing of up to 44 times. All of the information combined will allow for better-understood future work with both different eutectics and different biopolymers.

Future work may entail an expansion into larger nucleotides chains, potentially reaching gene length polymers on the order of hundreds of base pairs in length. Enzymatic studies can also be pursued to observe under what conditions of eutectic DNA-related enzymes such as ligases or polymerases can operate effectively. The behavior of catalytic nucleotides such as ribozymes may also prove interesting, as it can be seen that the general secondary structure is retained in the eutectic when compared to buffer, and therefore enzymatic activity may therefore also be retained, which could provide an alternative to protein based enzymes for use in such eutectic solvents as seen here.

APPENDIX

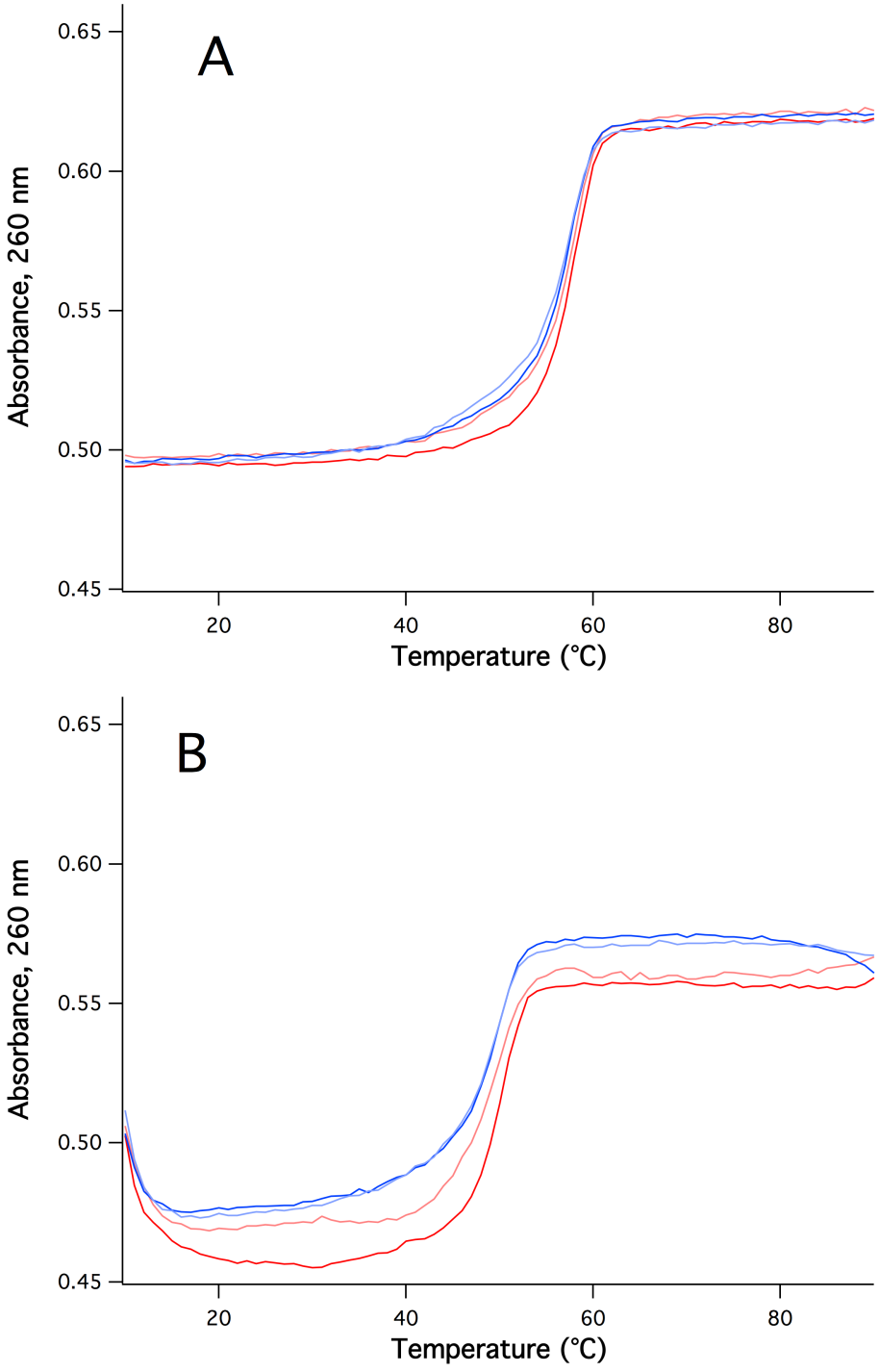
A
B
Absorbance, 260 nm
Temperature (°C)
0.65
0.60
0.55
0.50
0.45
20
40
60
80

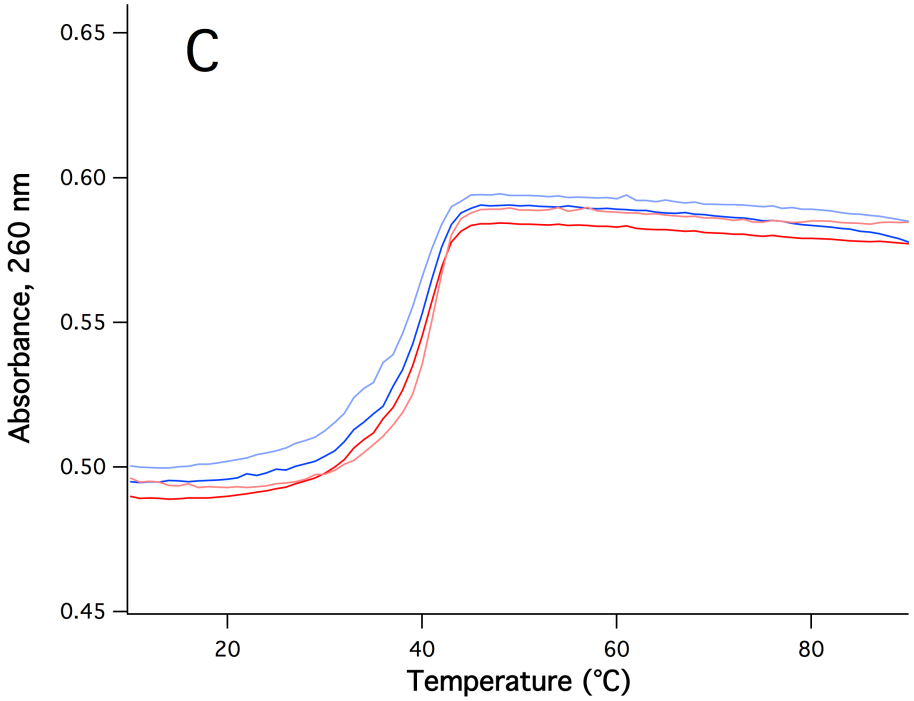
C
0.65
0.60
0.55
0.50
0.45
Absorbance, 260 nm
20
40
60
80
Temperature (°C)

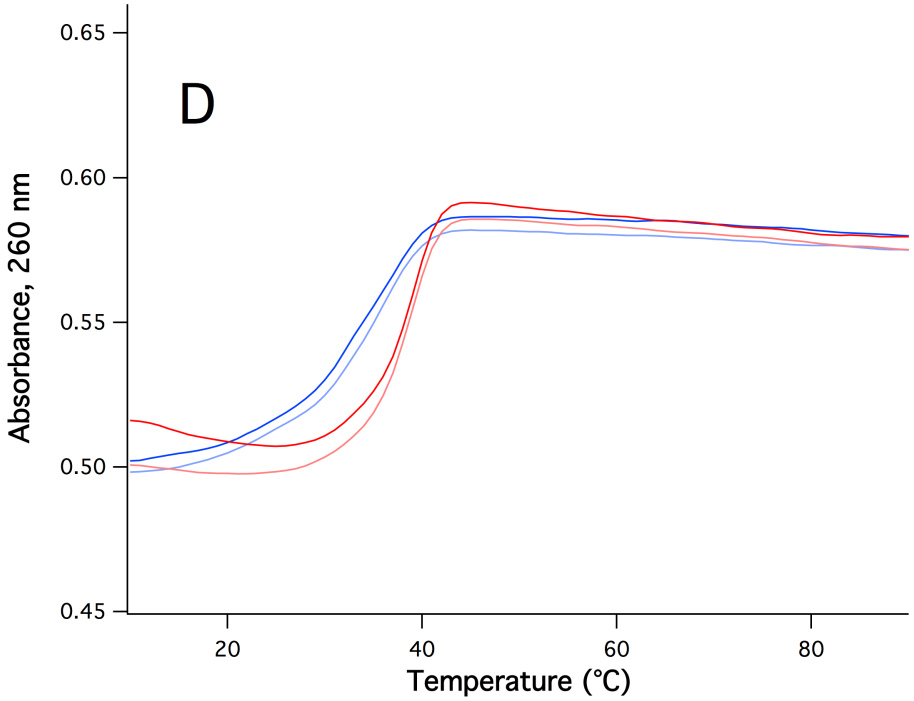
D
0.65
0.60
0.55
0.50
0.45
Absorbance, 260 nm
20
40
60
80
Temperature (°C)

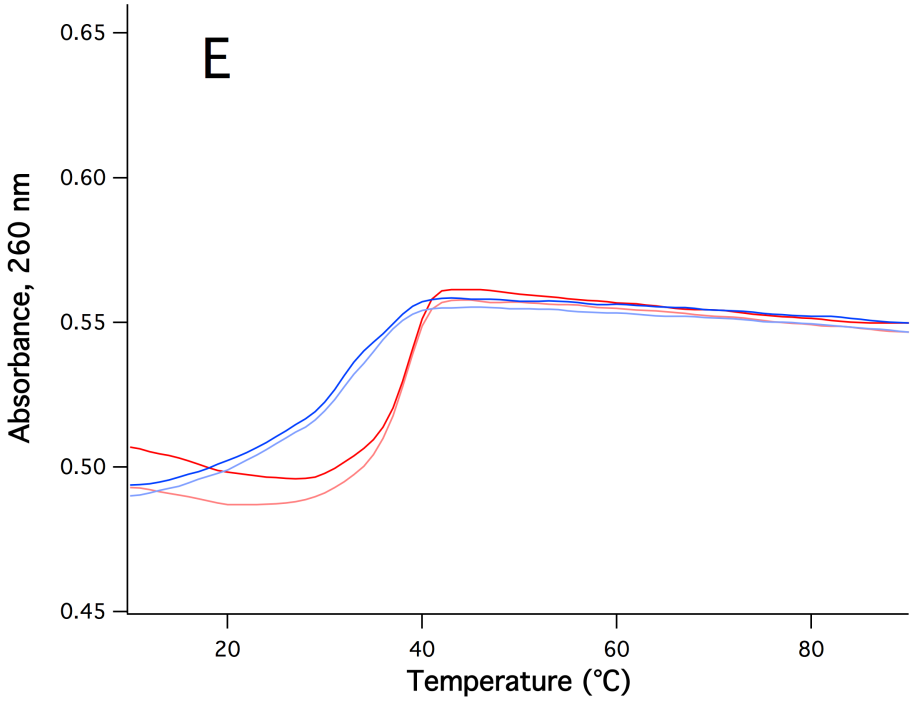
E
0.65
0.60
0.55
0.50
0.45
Absorbance, 260 nm
20
40
60
80
Temperature (°C)

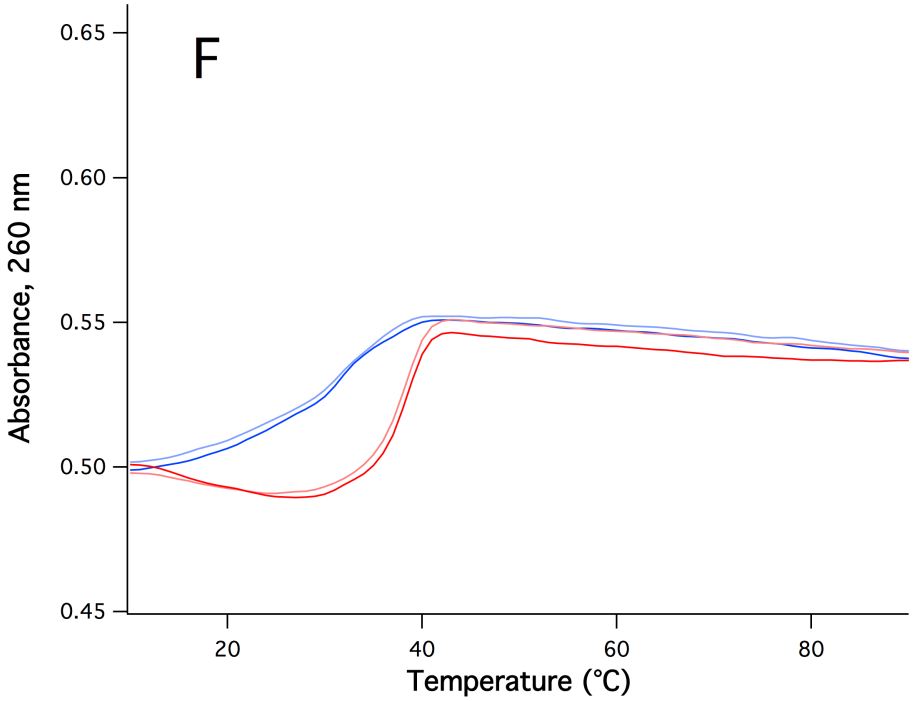
F
0.65
0.60
0.55
0.50
0.45
Absorbance, 260 nm
20
40
60
80
Temperature (°C)

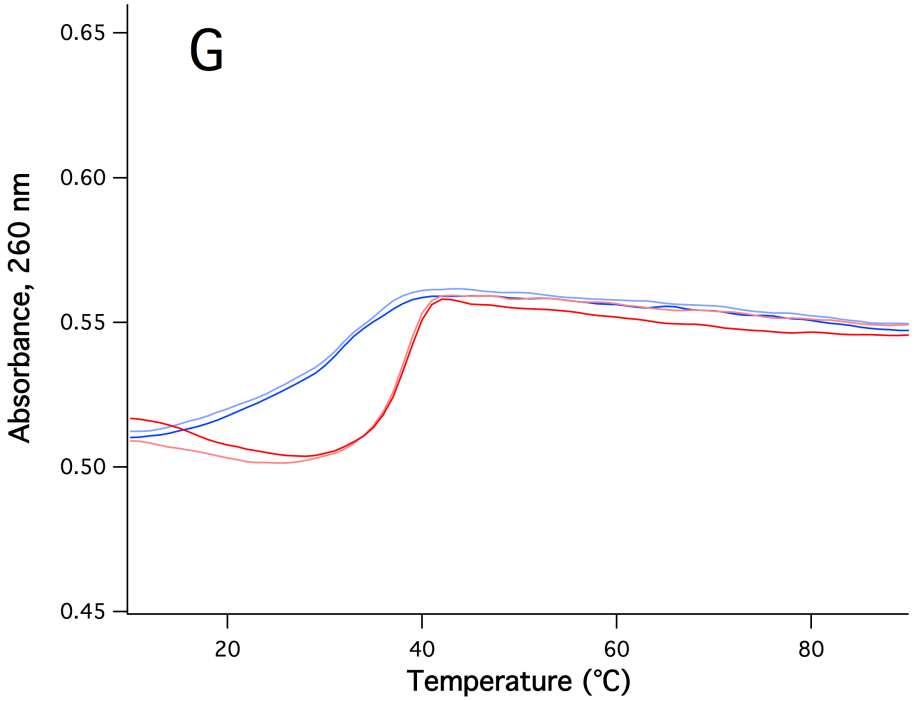
G
0.65
0.60
0.55
0.50
0.45
Absorbance, 260 nm
20
40
60
80
Temperature (°C)

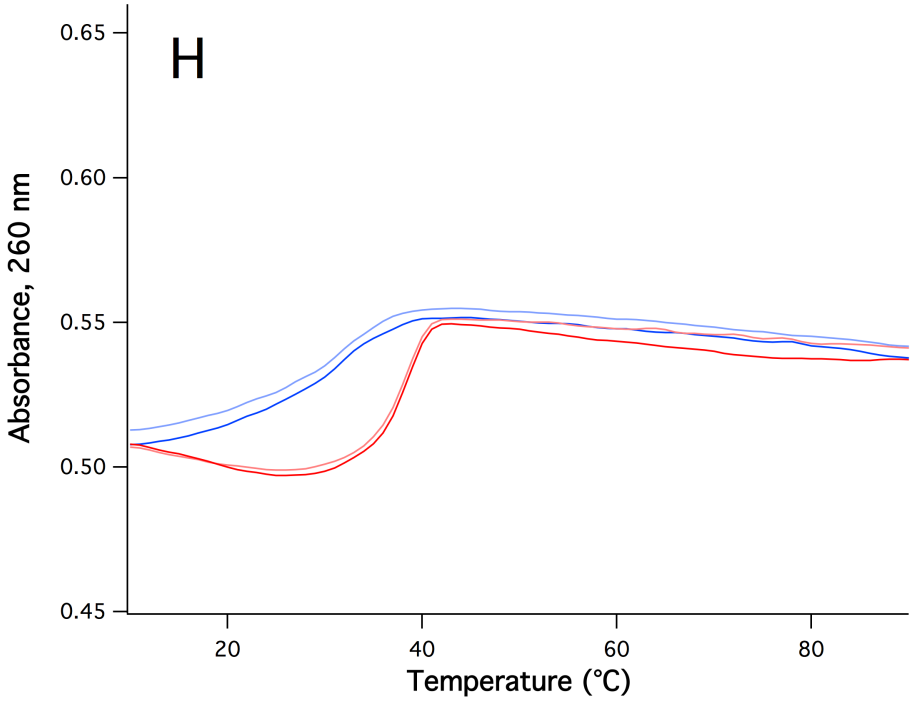
H
0.65
0.60
0.55
0.50
0.45
Absorbance, 260 nm
20
40
60
80
Temperature (°C)

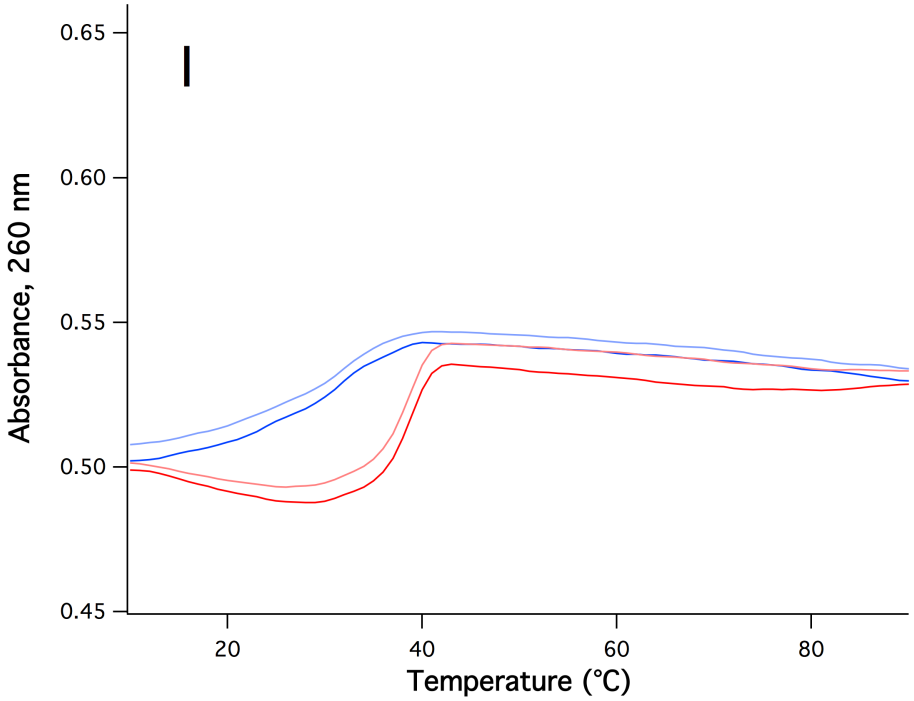

Appendix 1.1 Melts of 12.36 μM by strand 32-mer in varying dilutions of glycerol with 20 mM sodium phosphate pH 7 by mol: A, 5%, B, 20%, C, 50%, D, 65%, E, 80%, F, 90%, G, 93%, H, 97%, I, 100%. Red curves are heating traces, while blue curves are cooling traces.

REFERENCES

[1] Maltseva T.V., Agback P., Chattopadhyaya J., *How Much hydration is necessary for the stabilisation of the DNA-duplex?*, Nucleic Acids Research, 1993, 21, 4246-4252

[2] Abe H., Abe N., Shibata A., Ito K., Tanaka Y., Ito M., Saneyoshi H., Shuto S., Ito Y, *Structure Formation and Catalytic Activity of DNA Dissolved in Organic Solvents*, Angewandte Chem. Int. Ed., 2012, 51, 6475-6479

[3] Richmond TJ, Davey CA, et al, *The Structure of DNA in the nucleosome core*, Nature, 423, 145-150

[4] Benner S., Ricardo A., Carrigan M., *Is there a common chemical model for life in the universe?,* Current Opinions in Chemical Biology, 2004, 8, 672–689

[5] Hud N., Cafferty B., Krishnamurthy R., Williams L., *The Origin of RNA and ''My Grandfather's Axe''*, Chemistry & Biology, 2013, 20, 466-474

[6] Mamajanov I., Engelhart A., Bean H., Hud N., *DNA and RNA in Anhydrous Media: Duplex, Triplex, and G-Quadruplex Secondary Structures in a Deep Eutectic Solvent*, Angewandte Chemie, 2010, 122, 36, 6454 –6458

[7] Abbott A., Harris R., Ryder K., D'Agostino C., Gladden L., Mantle M., *Glycerol Eutectics as Sustainable Solvent Systems*, Green Chemistry, 2011, 13, 82-90

[8] Mondal D., Sharma M., Mukesh C., Gupta V., Prasad K., *Improved solubility of DNA in recyclable and reusable bio-based deep eutectic solvents with long-term structural and chemical stability*, Chemical Communications, 2013, 49, 9606-9608

[9] Sikorav J., Orland H., Braslau A., *Mechanism of Thermal Renaturation and Hybridization of Nucleic Acids: Kramers' Process and Universality in Watson–Crick Base Pairing*, Journal of Physical Chemistry B, 2009, 113, 3715-3725

[10] Lannan FM., Mamajanov I., Hud N., *Human telomere sequence DNA in water-free and high-viscosity solvents: G-quadruplex folding governed by Kramers rate theory*, Journal of the American Chemical Society, 2012, 134, 37, 15324-15330

[11] Yadav K., Trivedi S., Rai R., Pandey S., *Densities and dynamic viscosities of (choline chloride + glycerol) deep eutectic solvent and its aqueous mixtures in the temperature range (283.15–363.15)*, Fluid Phase Equilibria, 2014, 367, 135-142

[12] Zhang Q., Vigier K., Royer S., François J., *Deep eutectic solvents: syntheses, properties and applications*, Chemical Society Reviews, 2012, 41, 7108–7146

[13] Zhao C., Qu X., *Recent progress in G-quadruplex DNA in deep eutectic solvent*, Methods, 2013, 64, 1, 52–58

[14] Klibanov A., Bonner G., *Structural Stability of DNA in Nonaqueous Solvents*, Biotechnology and Bioengineering, 2000, 68, 3, 339–344

[15] Thomas R., *The denaturation of DNA*, Gene, 1993, 135, 1, 77-79

[16] Mergny J., Lacroix L., *Analysis of Thermal Melting Curves, Oligonucleotides*, 2003, 13, 515-537

[17] Puglisi J.D., Tinoco I. Jr., *Absorbance melting curves of RNA*, Methods in Enzymology, 1989, 180, 304–325.

[18] Dickerson R., Drew H., Conner B., Wing R., Fratini A., Kopka M., *The Anatomy of A-, B-, and Z-DNA*, Science, 216, 475-485.

[19] Saenger W., Hunter W., Kennard O., *DNA Conformation is determined by economics of hydration of phosophate groups*, Nature, 1986, 324, 385-388

[20] Kypr J., Kejnovská I., Renčiuk D., Vorličková M., *Circular dichroism and conformational polymorphism of DNA*, Nucleic Acids Research, 2009, 37, 6, 1713–1725

[21] Portella G., Germann M., Hud N., Orozco M., *MD and NMR Analyses of Choline and TMA Binding to Duplex DNA: On the Origins of Aberrant Sequence-Dependent Stability by Alkyl Cations in Aqueous and Water-Free Solvents*, Journal of the American Chemical Society, 2014, 136, 3075−3086

[22] Yamada M., Nomizu M., Satoh S., Ohkawa K., Yamamote H., Nishi N., D*NA with γ-Aminopropyltriethoxysilane Switches between B- and C-Form Structures under Thermal Control*, ChemBioChem, 2003, 4, 2-3, 232–234

[23] Wyer J., Kristensen M., Jones N., Hoffmann S., Nielsen S., *Kinetics of DNA duplex formation: A-tracts versus AT-tracts*, Physical Chemistry Chemical Physics, Advance Article, DOI: 10.1039/c4cp02252a.

[24] Wang S., Friedman A., Kool E., *Origins of High Sequence Selectivity: A Stopped-Flow Kinetics Study of DNA/RNA Hybridization by Duplex- and Triplex-Forming Oligonucleotides*, Biochemistry, 1995, 34, 9774-9784

[25] Gao Y., Wolf L., Georgiadis R., *Secondary structure effects on DNA*

hybridization kinetics: a solution versus surface comparison, Nucleic Acids Research, 2006, 34, 11, 3370–3377

[26] Wetmur J., *Hybridization and Renaturation Kinetics of Nucleic Acids*, Annual Review of Biophysics and Bioengineering, 1976, 5, 337-361

[27] Schmitz K., Schurr J., *Role of orientation constraints and rotational diffusion in bimolecular solution kinetics,* Journal of Physical Chemistry, 1972, 76 (4), 534–545

[28] Subriana J., Doty P., *Kinetics of Renaturation of Denatured DNA. I. Spectrophotometric Results*, Journal of Molecular Biology, 1966, 4, 171-187

[29] Patzel V., Sczakiel G., *Length Dependence of RNA-RNA Annealing, Journal of Molecular Biology*, 1999, 294, 1127-1134

[30] Rothemund P., *Folding DNA to create nanoscale shapes and patterns*, Nature, 2006, 440, 297-302

[31] Lindahl T., *Instability and decay of the primary structure of DNA,* 1993, Nature, 362, 709-715.

[32] Rauzan B., McMichael E., Cave R., Sevcik L., Ostrosky K., Whitman E., Stegemann R., Sinclair A., Serra M., Deckert A., *Kinetics and Thermodynamics of DNA, RNA, and Hybrid Duplex Formation*, Biochemistry, 2013, 52, 765-772

[33] Gosule L., Schellman J., *Compact form of DNA induced by spermidine*, Nature, 1976, 259, 333-335

[34] Huang Z., Wu B., Wen Q., Yang T., Yang Z., *Deep eutectic solvents can be viable enzyme activators and stabilizers*, Journal of Chemical Technology and Biotechology, 2013, DOI: 10.1002/jctb.4285

[35] Baase W., Johnson Jr. W., *Circular dichroism and DNA secondary structure.*, Nucleic Acids Research, 1979, 6, 2, 797-814.

[36] Benner S., Kim H., Yang Z., *Setting the Stage: The History, Chemistry, and Geobiology behind RNA*, Cold Spring Harbor Perspectives in Biology, 2010, DOI: 10.1101/cshperspect.a003541

[37] Thrower K., Peacocke A., *Kinetic and Spectrophotometric Studies on the Renaturation of Deoxyribonucleic Acid,* Biochemistry Journal, 1968, 109, 543-556

[38] Peterson A., Heaton R., Georgiadis R., *The effect of surface probe density on DNA hybridization, Nucleic Acids Research*, 2001, 29, 5163-5168

[39] Chan, V; Graves, DJ; McKenzie, SE, *The biophysics of DNA hybridization with immobilized oligonucleotide probes*, Biophysical Journal, 1995, 69, 2243-2255

[40] Wieder R., Wetmur J., *One Hundred-Fold Acceleration of DNA Renaturation Rates in Solution*, Biopolymers, 1981, 20, 1537-1547

[41] Thomas R., *Sur l'existence, dans la molécule des acides nucléiques, d'une structure secondaire à liaisons labiles*, Experientia, 1951, 7, 261-262

[42] Hud NV, Plavec J, *A unified model for the origin of DNA sequence-directed curvature*, Biopolymers, 2003, 69, 1, 144-159

[43] Nakano M, Tateishi-Karimata H, Tanaka S, Sugimoto N, Choline Ion *Interactions with DNA Atoms Explain Unique Stabilization of A-T Base Pairs in DNA Duplexes: A Microscopic View*, Journal of Physical Chemistry B, 2013, 118, 2, 379-389

[44] Finch, A, Anton C, Jacob C, et al, *Assembly of DNA Architectures in a Non-Aqueous Solution*, Nanomaterials, 2012, 3, 275-285

[45] Zhao H, Baker G, Holmes S, *New eutectic ionic liquids for lipase activation and enzymatic preparation of biodiesel*, Organic & Biomolecular Chemistry, 2011, 9, 6, 1908-1916